NATIONAL ADVISORY COMMITTEE FOR AERONAUTICS

TECHNICAL NOTE 4329

INFLUENCE OF HEAT TREATMENT ON MICROSTRUCTURE AND HIGH-TEMPERATURE PROPERTIES OF A NICKEL-BASE PRECIPITATION-HARDENING ALLOY

By R. F. Decker, John P. Rowe, W. C. Bigelow, and J. W. Freeman

University of Michigan

Washington

July 1958

NATIONAL ADVISORY COMMITTEE FOR AERONAUTICS

TECHNICAL NOTE 4329

INFLUENCE OF HEAT TREATMENT ON MICROSTRUCTURE AND HIGH-TEMPERATURE PROPERTIES OF A NICKEL-BASE PRECIPITATION-HARDENING ALLOY

By R. F. Decker, John P. Rowe, W. C. Bigelow, and J. W. Freeman

SUMMARY

Studies have been made of the influence of various heat treatments on the rupture properties and microstructure of a 55Ni-20Cr-15Co-4Mo-3Ti-3Al alloy to provide more fundamental information on the relationships between structure and high-temperature properties in alloys of this type. The effects of variations in solution treatment, cooling rate after solution treatment, and aging treatment on the stress-rupture properties of the alloy at 1,600° F and 25,000 psi have been measured and related to variations in the size and distribution of precipitates within the alloy and to residual rolling effects.

The temperature for complete solution of precipitates was found to lie between 1,975° and 2,000° F, and the temperature at which the alloy was solution-treated was found to have a marked effect on its stress-rupture properties. Solution treatment at 1,975° F resulted in a shorter rupture life than that produced by treatment at 2,150° F or treatment at 2,150° F followed by treatment at 1,975° F. The experimental evidence indicates that this was not due to the lack of complete solution of the γ' phase but to the fact that residual effects from prior rolling operations remained in the alloy when the 1,975° F solution treatment alone was used.

Cooling rate after solution treatment also affected subsequent stress-rupture properties of the alloy. The extremely rapid and extremely slow cooling methods, ice-brine-quenching and furnace-cooling, resulted in rupture properties which were inferior to those achieved by a moderate cooling method, air-cooling. These effects were related to the distribution of the γ' phase. Furnace-cooling caused overaging with a coarse dispersion of agglomerated γ' particles while ice-brine-quenching induced considerable cellular precipitation of the γ' phase at the grain boundaries. The inferior properties after these treatments are considered to be manifestations of these overaging phenomena.

Double-aging treatments after solution treatment had no significant effect on stress-rupture properties. Qualitative comparisons were made of the effects of isothermal aging with and without application of stress. No significant difference was noted in the rate at which precipitation of the γ' phase proceeded within the matrix grains. In general, the rate of localized precipitation at the grain boundaries was also similar at part of the grain boundaries; but there appeared to be a higher incidence of severe overaging and agglomeration in restricted portions of grain boundaries in the specimens aged under stress.

In general, it was concluded that the stress-rupture properties of the alloy could be related to the size and dispersion of the γ' particles, provided that residual rolling effects were removed by the solution treatment. The heat treatments which left finely dispersed γ' particles throughout the microstructure gave essentially equal properties at 1,600° F and 25,000 psi. Heat treatments which caused overaging in the matrix or at the grain boundaries before testing led to significantly lower high-temperature properties.

INTRODUCTION

It is generally accepted that the favorable high-temperature properties of the nickel-base alloys hardened by titanium and aluminum result from the precipitation of the intermetallic γ' phase within the matrix of the alloy. The γ' phase has been shown to have a face-centered cubic structure similar to that of the Ni_3Al phase of the nickel-aluminum system with a lattice parameter closely matched to that of the matrix of the alloys (refs. 1 and 2). Compositionally, the phase has been shown to dissolve titanium and is frequently referred to as $Ni_3(Al, Ti)$. The heat resistance of these alloys has been attributed to the presence of γ' particles (refs. 1, 3, and 4) and to the fact that the γ' phase forms in fine dispersion within the matrix; however, attempts to relate the distribution of the γ' particles with the metallurgical properties have been only moderately successful to date.

Frey, Freeman, and White (ref. 5) and subsequently Brockway and Bigelow (ref. 6) found that the dispersion of the γ' particles in Inconel X alloy correlated with stress-rupture properties at 1,200° F, which was low in the aging range for this alloy; however, no correlation was obtained for rupture tests at 1,500° F, which was high in the aging-temperature range and which produced rapid aging during testing. Betteridge and Smith (ref. 7) studied the relation between structure and creep properties of Nimonic alloys tested high in the aging range. They found that highest stress-rupture properties were obtained with the greatest volume percent of γ' particles and showed that usefulness

of conventional aging was clearly decreased when test temperature was greater than 1,600° F. The absence of a discontinuity in the curve of rupture strength against temperature in the region of the temperature at which the γ' phase was completely soluble was interpreted as showing that rupture strength was a consequence of both precipitation and solid-solution hardening. This is in agreement with the theories of Geisler (ref. 8) on the effect of age hardening on deformation resistance of the alloy and with his proposal that the depletion of solid-solution hardeners by overaging can reduce deformation resistance to that of the solution-treated alloy.

In order to extend knowledge of the nickel-base alloys to the higher titanium and aluminum levels now in use, a study of the effect of heat treatment upon properties of a 55Ni-20Cr-15Co-4Mo-3Al-3Ti alloy has been undertaken with the objectives of establishing the important variables in heat-treating practices and determining the fundamental metallurgical mechanisms by which these variables influence the properties of the alloy. This has been part of an extensive program at the University of Michigan studying the basic mechanisms by which processing variables influence high-temperature properties of nickel-base heat-resistant alloys hardened with titanium and aluminum. The present report describes studies of the influence of selected heat treatments on the rupture properties of this alloy at 1,600° F and the progress which has been made to date in relating these properties to the microstructures of the alloy.

The investigation was conducted at the Engineering Research Institute of the University of Michigan under the sponsorship and with the financial assistance of the National Advisory Committee for Aeronautics. The authors would like to acknowledge the invaluable contribution of a number of people who have assisted on this project. Professor C. C. Craig supplied valuable advice about the statistical analysis included in the appendix, Mr. Karl Kienholz operated the University of Michigan vacuum-melting furnace in the processing of the experimental heats, and Mr. Jerry White assisted in hot-working and heat-treating many of the samples. Mr. Alex Dano's development of etching procedures for both macroscopic and optical-microscopic work was instrumental in the completion of the microstructural studies and his utilization of careful and precise techniques resulted in the electron micrographs shown in the report. Miss Christine Sadler prepared many of the metallographic samples and photographs. Mr. George Hynes and Mr. Dick Umstead ran the stress-rupture tests.

EXPERIMENTAL PROCEDURES

Material

The experiments were conducted on an alloy of the composition shown below:

Chemical composition, weight percent

Cr	Co	Mo	Ti	Al	Mn	Si	Fe	Zr	C	B	S	Ni
18.8	15.1	4.15	3.14	3.14	<0.10	0.10	<0.30	0.19	0.08	0.0005	0.008	Balance

This heat was melted in the University of Michigan vacuum-melting furnace from virgin stock in a zirconia crucible and was cast into a 10-pound ingot of 2.5-inch diameter. As-cast structures of the alloy are shown in figure 1. The ingot was homogenized 1 hour at 2,300° F, air-cooled, surface-ground, and rolled to 7/8-inch bar stock using 22 passes of approximately 7-percent reduction each, with 10-minute reheats between passes. The resulting as-rolled bar stock and its microstructure are illustrated in figure 2.

Metallography

All metallographic samples were mechanically polished with 3/0 paper and then electropolished in a solution of 10 parts of 70 percent perchloric acid and 90 parts of glacial acetic acid. Electropolishing was carried out at approximately 30 volts with a current density of 0.8 ampere per square inch. Cyclic polishing of 5 seconds on and 5 seconds off was employed for a total period of electrolysis of about 30 seconds.

Samples for optical microscopy were etched with etchant A (see table I) at 1 to 6 volts with a current density of 0.1 to 0.5 ampere per square inch for 5 to 15 seconds, depending upon the condition of the stock.

Etching for all except one of the electron microstructures was accomplished with a procedure developed by Bigelow, Amy, and Brockway (ref. 9) with etchant B (see table I) using 6 volts and a current density of 0.8 ampere per square inch for periods of 3 to 7 seconds. This etching procedure selectively attacks the matrix, leaving the

γ' phase protruding from the sample surface. In order to reveal the two-phase composition of the precipitates at the grain boundaries of one of the samples, etchant B was diluted by a water addition equal to 15 percent by volume of the original etchant and this diluted etchant was designated as etchant C (see table I). Etchant C causes the carbides to protrude from the sample surface more than the γ' phase protrudes.

For electron microscopy, collodion replicas of the metallic surface were used. These were shadowed with palladium to increase contrast and reveal surface contours; polystyrene latex spheres approximately 2,580 angstrom units in diameter were placed on the replicas prior to shadowing to indicate the angle and direction of shadowing and to provide an internal standard for measurement of magnification. The micrographs reproduced in this report are copies of direct prints from the original negatives; consequently, the polystyrene spheres appear black and the shadows formed by the palladium appear white.

Hardness

Vickers penetration hardness measured in Vickers pyramid number (VPN) was measured with a 50,000-gram load. Three impressions were made on each sample, both diagonals of each impression being measured. Statistical analysis of testing variability (see appendix) established that in the range of 300 to 340 VPN a hardness difference of 7 VPN was significant while in the range of 340 to 400 VPN a hardness difference of 9 VPN was significant.

X-Ray Diffraction

The X-ray diffraction studies were made on selected samples to detect the presence of the γ' phase. Samples etched as for electron micrography were affixed on a rotating specimen mount at the center of a Debye-Scherrer type camera with incident beam at an angle of 20° to the surface. Chromium K radiation was used to give maximum separation of the diffraction lines and to minimize fluorescence effects.

Stress-Rupture Testing

High-temperature properties were evaluated by stress-rupture tests at $1,600^{\circ}$ F and 25,000 psi using 0.250-inch-diameter specimens machined from heat-treated bar stock. The specimens were preheated 4 hours at $1,600^{\circ}$ F in the rupture units before the loading.

RESULTS

The studies of the effect of thermal treatments on the size and distribution of precipitates and on high-temperature properties can be categorized as: (1) Study of effect of solution-treating temperature, (2) study of effect of cooling rate after solution treatment, and (3) study of isothermal aging after solution treatment. The results and discussion will be presented in this order below. The initial microstructures of the rupture samples are presented in figure 3, and the results of rupture tests are plotted on a rupture band in figure 4 and listed in table II. Table III gives the hardness data of the heat-treated samples.

Effect of Solution-Treating Temperatures

In order to establish the minimum temperature for complete solution of the precipitates in 4 hours, specimens which had been treated 2 hours at 2,150° F and air-cooled were subsequently treated 4 hours at 1,700°, 1,800°, 1,900°, and 2,000° F and ice-brine-quenched. The initial 2-hour treatment was applied to homogenize the as-rolled structure.

The micrographs of figures 5(a), 5(b), and 5(c) show a uniform distribution of the γ' particles throughout the matrix of the alloy. Following the convention of Geisler, this will be referred to henceforth as "general precipitate." From micrographs it appears that the size of the particles increased but that the volume percent of the phase decreased up to 1,900° F. The γ' particles were not evident after treatment at 2,000° F (fig. 5(d)).

In the electron micrographs there is some evidence that two phases agglomerated in the grain boundaries during treatment at 1,700°, 1,800°, and 1,900° F. Particles of one phase were surrounded by a second agglomerated phase. Selective etching techniques showed that the surrounding phase etched like the general precipitate of γ' phase. The surrounded particles were distributed less uniformly in the boundaries and are assumed to be carbides.

The X-ray diffraction data obtained provided evidence that γ' particles were present in the sample treated at 1,900° F; however, γ' particles were not detected in the sample treated at 2,000° F (see table IV). This is consistent with the observations on the microstructure described above. Microstructural studies also showed that the solution of the γ' phase was not complete at 1,975° F. This was indicated by the occurrence of very large γ' particles, similar to those in the specimen treated at 1,900° F, in a specimen which was treated 2 hours at

2,150° F, then reheated 4 hours at 1,975° F (see fig. 3(c)). The presence of the numerous very small γ' particles shown in figure 3(c) in addition to these large particles is attributed to the fact that the specimen was air-cooled following the treatment at 1,975° F.

The hardness measurements (fig. 6) confirm the microstructural findings in an indirect way. As the heat-treating temperature was increased to 1,900° F, hardness decreased. The hardness after treating at 2,000° or 2,150° F was, however, significantly higher than the value for 1,900° F.

There are believed to be two mechanisms to account for this latter increase in hardness. It could be that matrix solid-solution hardening resulted from dissolving the precipitates (γ' and/or carbides), or that the more complete solution of precipitates obtained at 2,000° F created a greater driving force for reprecipitation of the γ' phase during the ice-brine-quenching treatment. Regardless, the true hardness indicator of the solution temperature seems to be the sharp increase of hardness between 1,900° and 2,000° F.

This definitely established the temperature for complete solution of the γ' phase in this alloy as lying between 1,975° and 2,000° F for a 4-hour treatment. These results are in good agreement with the results of Betteridge and Franklin (ref. 3) on Nimonic alloys containing titanium and aluminum in a 2-to-1 ratio if it is assumed that the total percent of Ti plus Al is the factor determining the solution temperature. The solution temperature they observed for an alloy containing a total of 6.3 percent Ti and Al was in the same range as observed here with a comparable Ti and Al content as shown in figure 7.

The micrographs do not show appreciable grain-boundary precipitation in specimens treated in the range of 1,975° to 2,000° F, which indicates that the carbides which generally form at the grain boundaries also dissolve.

In order to find the effect of solution treatment on their high-temperature stress-rupture properties, as-rolled samples were heat-treated and rupture-tested at 1,600° F and 25,000 psi. The results are shown in table II and microstructures of specimens after testing are shown in figures 8 and 9. The rupture life for the specimen treated only at 1,975° F was considerably less than that for the specimens treated at 2,150° F, and this difference is considered to indicate a significant difference in properties as shown in the appendix. Conversely, the ductility of the specimen treated only at 1,975° F was higher than that of the specimen treated at 2,150° F.

It is apparent from the microstructures that heat treatment at 1,975° F left a coarse precipitate of γ' particles. Micrographs of the sample treated only at 1,975° F revealed a grain structure with some nonuniformity of grain size and a banded distribution of undissolved γ' particles. In addition, the microstructure after testing showed the presence of many small areas where overaging occurred during testing (cf. figs. 3(a) and 8). The high hardness of this sample before testing also indicated that residual rolling effects were present. The double treatment at 2,150° and 1,975° F removed these rolling effects, as evidenced by the lowered hardness, but left residual precipitation (see fig. 3(c)).

The optical micrographs of figures 3(a) and 3(c) indicate two types of banding in the specimens: The narrow banding running generally parallel to the direction of rolling (see fig. 3(c)) and the broader banding running at an angle to the fine bands (see fig. 3(a)). These latter bands are thought to be produced by precipitation of larger particles of γ' phase in regions of residual stresses resulting from rolling operations. The finer bands are thought to indicate inhomogeneities in the distribution of the titanium and aluminum in the alloys.

Knowledge of these observations allows one to analyze the stress-rupture results from the study of effect of solution treatment on high-temperature properties. A clearly significant increase in rupture life resulted from including a treatment at 2,150° F in the heat treatment after rolling. When treatments at either 2,150° F or 2,150° F plus 1,975° F were used, the rupture life was significantly higher than when only the treatment at 1,975° F was used.

It can be postulated that one or both of two causes operated here: (1) Incomplete removal of residual working effects from rolling, and/or (2) incomplete solution of the γ' phase. The fact that the treatment at 2,150° plus 1,975° F (with incomplete solution of γ' particles) gave essentially the same rupture life as the 2,150° F treatment (with complete solution of γ' particles) indicates that the second cause was not governing. Then it is apparent that the 1,975° F treatment was inferior because it did not completely remove the residual rolling effects. The inhomogeneous structure and high hardness after the solution treatment support this conclusion.

In hot-rolling work on alloys of this type it has often been found that residual rolling effects are not removed by a 4-hour treatment at 1,975° F. Removal of effects from working at 2,150° F can require several minutes of reheat time at 2,150° F. Evidently, the residual effects alter the aging reaction during subsequent testing and lower the rupture life.

Effect of Cooling Rate After Solution Treatment

It has been established by Dennison (ref. 10) that cooling rate after solution treatment has a marked influence on subsequent high-temperature properties of some age-hardening alloys. Specifically, in alloys which were subject to localized grain-boundary precipitate or cellular precipitation, furnace-cooling resulted in superior properties in comparison with those produced by the faster rates of cooling. To study the effects of cooling rates on the properties of the present alloy, metallographic specimens and rupture specimens were prepared using ice-brine-quenching, air-cooling, and furnace-cooling after a solution treatment of 2 hours at 2,150° F. In addition, one metallographic specimen was water-quenched. Figure 10 shows the microstructures and hardnesses of these samples. The electron micrographs show that rapid precipitation of the γ' phase occurred when the alloy was air-cooled or furnace-cooled, but no such precipitation was resolved after water-quenching or ice-brine-quenching. Neither the optical nor the electron micrographs revealed much localized precipitation at the grain boundaries after any of these treatments.

The relatively high hardness of the air-cooled specimen correlates with the microstructural evidence of a fine dispersion of the γ' particles within the matrix, and the relatively low hardness of the furnace-cooled specimen correlates with the fact that micrographs show a greatly overaged condition of the γ' particles. The fact that the hardness of the water-quenched specimen is slightly greater than that of the ice-brine-quenched specimen suggests the occurrence of an extremely fine dispersion of γ' particles which are not resolved by the electron micrographs. Such a fine dispersion may also exist in the ice-brine-quenched specimen to account for its hardness of 313 VPN, which is surprisingly high for a fully solutioned alloy of this type.

In order to establish the effect of cooling rate after solution treatment on their high-temperature stress-rupture properties, samples were rupture-tested at 1,600° F and 25,000 psi. The complete specimen treatments and test results are given in table II and microstructures of the specimens after testing are shown in figures 9 and 11 to 13.

Comparison of the results with treatments D and E (see table II) indicates that ice-brine-quenching had a very deleterious effect on both rupture life and ductility. Comparison of the results with treatments B and F reveals that furnace-cooling resulted in a rupture life significantly lower than that produced by air-cooling (see appendix). The slight improvement in ductility after furnace-cooling was probably not statistically significant.

In comparing the microstructures after testing of the ice-brine-quenched and aged sample with those of the air-cooled and aged sample (see figs. 11 and 12), one observes differences in both the general precipitation and the localized precipitates at the grain boundaries. The differences in general precipitate size can be attributed to the fact that the test time allowed more aging in the air-cooled sample. The differences in localized precipitates are considered most significant. The air-cooled and double-aged sample exhibited massive γ' particles (from the 1,975° F treatment) and some carbides at the grain boundaries while the ice-brine-quenched and aged sample had undergone cellular precipitation at some boundaries. It is believed that this cellular precipitate formed during aging prior to loading as a result of residual strains induced at the grain boundaries by the ice-brine-quenching and was related to the brittle, weak characteristics of the ice-brine-quenched sample. This is consistent with the conclusions of Roberts (ref. 11) that plastic deformation favored cellular precipitation over general precipitation in magnesium-aluminum alloys because of buildup of elastic-strain energy at the boundaries and that their comparatively poor elevated-temperature creep properties accompanied the presence of the cellular precipitation which allowed easy deformation at the grain boundaries. Dennison (ref. 10) also observed that cellular precipitation invariably resulted in low ductilities and low rupture strengths in copper-aluminum alloys with additions of cobalt, nickel, and iron because of rapid, brittle fracture through the grain boundaries.

Air-cooling after solution treatment precipitated a finer dispersion of γ' particles than those produced by furnace-cooling, which resulted in a coarse general precipitate (see fig. 10). The essential feature here is the comparison of the probable precipitate size at the time of rupture-test loading after the 4-hour preheat at 1,600° F. Microstructures taken of aged specimens in the following study of aging suggest that the air-cooled sample was overaged. Therefore, it is probable that the inferiority of the furnace-cooled condition resulted from the overaging of the γ' precipitate. It is entirely possible that a cooling rate intermediate to air-cooling and furnace-cooling would improve rupture life over that of the furnace-cooled condition.

Effect of Isothermal Aging After Solution Treatment

Studies of the effects of isothermal aging on microstructure and hardness were made with samples aged 1, 10, and 100 hours at 1,000°, 1,200°, and 1,400° F and 1, 4, 10, and 100 hours at 1,600° F. Two initial conditions were used for each of these aging conditions: Solution treatment for 2 hours at 2,150° F followed by air-cooling, and solution treatment for 2 hours at 2,150° F followed by ice-brine-quenching. These conditions differed in that considerable precipitation

of the γ' phase occurred during air-cooling, whereas ice-brine-quenching gave a more precipitate-free condition prior to aging.

Hardness curves for the aged specimens are plotted in figures 14 and 15. These curves show several interesting general trends in development of hardness which appear to be independent of prior cooling rate:

(1) Aging at 1,000° F increased hardness little.

(2) Hardness increased progressively up to 100 hours at 1,200° and 1,400° F with no apparent overaging.

(3) Overaging occurred at 1,600° F after about 4 hours.

In addition, comparison of figures 14 and 15 shows several trends which apparently resulted from the differences in the initial treatment before aging:

(1) Hardness increased more rapidly at 1,200° and 1,400° F after ice-brine-quenching than after air-cooling.

(2) The difference in the initial precipitate present in the air-cooled and ice-brine-quenched conditions affected the aging curves at 1,000° and 1,200° F. Longer aging times were needed to reach a given hardness level when the initial condition was ice-brine-quenched.

(3) At 1,400° F, although the hardness after aging 1 hour was lower in the ice-brine-quenched sample, longer aging times gave approximately the same hardness level with both starting conditions.

(4) During aging at 1,600° F the samples initially ice-brine-quenched reached a higher hardness level and resisted overaging to a greater extent.

Representative micrographs of the aged samples are included in figures 16 through 18. It was observed from these that:

(1) The general γ' precipitate was not clearly resolvable by optical microscopy after any of the aging treatments. Aging did develop the precipitate so that evidence of it was seen in optical micrographs as a general greying or spotting of the background. The general γ' precipitate was resolved by electron microscopy in all samples aged at 1,400° and 1,600° F.

(2) Significant changes occurred in the grain boundaries during aging. In general, the grain boundaries broadened with increasing temperature and time at temperature. Localized precipitation and agglomeration of γ' particles at the boundaries were accompanied by

precipitation of another phase presumed to be a carbide. The duplex constitution of the boundaries was substantiated by etching techniques illustrated by figures 18(c) and 18(d). This finding is in agreement with that of Baillie and Poulignier (ref. 12), who found evidence for two phases at the grain boundaries of nickel-base alloys with one of the phases evolving and etching like the γ' phase.

(3) A cellular precipitation occurred at the grain boundaries during aging after ice-brine-quenching. This localized precipitation was most pronounced at 1,200° and 1,400° F and preceded general precipitation in the matrix. The particles in the cells appeared like γ' particles in electron micrographs.

(4) The electron micrographs indicated that the visible general precipitate changed little during aging at 1,000° and 1,200° F. Aging at 1,400° and 1,600° F after both initial treatments resulted in growth of the precipitate particles. In considering these overall results it is interesting to note that there is generally a good correlation between the size and distribution of the γ' particles and the hardness of the alloy. The general precipitate in the specimens which were air-cooled and subsequently aged 100 hours at 1,200° and 1,400° F (see figs. 17(b) and 17(c)) is very similar to that of the specimen which was ice-brine-quenched and aged 100 hours at 1,400° F (see fig. 16(c)) and all of these specimens have nearly the same hardness.

In order to establish the effect of aging after solution treatment prior to testing on their high-temperature stress-rupture properties, samples were prepared and tested at 1,600° F and 25,000 psi, as shown in table II.

By comparing results of treatments B and C with those of treatments G and E, respectively, it can be seen that no significant effect of aging prior to testing was found (see appendix). The microstructures before testing (see figs. 3(b), 3(c), 3(e), and 3(g)) show that all the samples had at that time a fine dispersion of γ' particles. For comparison, the microstructures after testing are shown in figures 9 and 12. It is probable that the 4-hour preheat time at 1,600° F before stressing acted as an equalizer. All the samples were probably aged to near maximum hardness and optimum precipitate dispersion, thereby masking the effect of prior aging.

Although the data showed that solution treatment at 2,150° F followed by air-cooling gave a rupture life comparable to that of an aged specimen, the results might have differed somewhat if different rupture-testing conditions and preheat time had been used. However, it suffices to state that the optimum rupture life will probably be obtained with a pretreatment which avoids grain-boundary overaging before testing and gives a dispersion of γ' particles aged near maximum hardness at the time of loading.

Cellular Precipitation

A high incidence of cellular precipitation was observed at the grain boundaries of specimens aged after ice-brine-quenching from the solution treatment, whereas the general tendency in specimens which were not ice-brine-quenched was for a more uniform agglomeration of the γ' and carbide phases. The development of the cellular precipitate in the grain boundaries was very rapid, and in the specimens aged at 1,200° F it preceded visible evidence of general precipitation of the γ' phase (see fig. 16(b)). In many cases the cellular particles seemed to nucleate at points in the matrix near the grain boundaries and then grow (see figs. 16(b) and 16(c)). The size of the γ' particles in the cells was usually large compared with that of those in the adjoining matrix, and the general condition within the cells appeared to be one of such extreme overaging that there was considerable precipitate-free matrix between the cellular particles.

It seems very possible that the driving force behind this accelerated cellular precipitation near the grain boundaries was thermal stressing. It is known that alloys of this type undergo plastic flow during quenching (ref. 13) resulting in residual strain energy. It is possible that the matrix material near the grain boundaries retained this strain energy after ice-brine-quenching and that this residual strain energy was sufficient to initiate the cellular precipitation during subsequent aging treatments.

Effect of Rupture Testing on Structures

The hardnesses of ruptured samples (aged under stress), except for the ice-brine-quenched and furnace-cooled samples, were essentially equal despite the differences in rupture time. They all were in the range of 362 to 368 VPN. This level was significantly higher than the hardness of 328 VPN for the sample aged 100 hours at 1,600° F with no stress applied. The microstructures revealed that the general precipitate size and distribution in the matrix corresponded roughly to that of samples aged without stress for a time corresponding to the rupture time. Therefore, stressing seemingly had no effect on the general precipitate size. However, stressing did prevent the hardness decrease which accompanied the overaging in the nonstressed aging samples. Evidently, an increment of hardness was added by the creep deformation which occurred during the rupture test.

The most striking difference between aged specimens and specimens aged under stress was at the grain boundaries. While part of the grain boundaries of the ruptured specimens closely resembled grain boundaries of aged specimens, the remainder were heavily overaged with large agglomerated γ' particles in fields of matrix which were otherwise precipitate

free. These observations are in agreement with those of Baillie and Poulignier (ref. 12) who found for similar nickel-base alloys that stress had little if any effect on general precipitation during aging but produced some changes at the grain boundaries.

DISCUSSION

One of the important contributions of this report is that it shows the microstructures developed in a typical nickel-base alloy under a variety of different heat treatments. The most striking microstructural characteristic of this type of alloy is the large amount of the intermetallic γ' phase which precipitates within the matrix grains and the rapidity with which it forms. For the 55Ni-20Cr-15Co-4Mo-3Ti-3Al alloy studied here, the temperature for complete solution of this phase was found to be between 1,975° and 2,000° F, and very rapid cooling by water or ice-brine-quenching was required after solution treatment to prevent reprecipitation of resolvable amounts of γ' phase. Short periods of aging at 1,400° to 1,600° F or air-cooling after solution treatment produce a very close dispersion of γ' particles which are only a few hundred angstrom units in diameter. Additional aging at these temperatures causes an increase in both the size and the separation of these particles. Aging at temperatures of 1,200° F and below for periods of as much as 100 hours appears to have little effect on the precipitation of the γ' phase, while aging for only a few hours at temperatures of 1,700° to 1,900° F produces severe overaging characterized by very large and widely separated particles. In all cases, except with furnace-cooling after solution treatment, these γ' particles appeared to be spheroidal in shape. It was particularly interesting to note that microstructures produced by aging under stress were very similar to those produced by comparable aging treatments without stress.

Precipitation at the grain boundaries consisted of two phases, one apparently a carbide phase and the other the γ' phase. Aging after air-cooling from solution treatment generally appeared to result in a gradual development of these phases at the grain boundaries with no particular evidence of depletion of the nearby matrix areas. This process was generally slow compared with the development of a cellular type of precipitation at a large fraction of the grain boundaries during aging after ice-brine-quenching. Cellular precipitation appeared to consist of rods or plates of the γ' phase extending outward from the grain boundaries and surrounded by depleted regions of matrix. The development of this condition was rapid compared with that of the matrix precipitation; aging 100 hours at 1,200° F after ice-brine-quenching from solution treatment produced extensive cellular precipitation but no detectable γ' particles in the matrix.

The observation of these microstructural characteristics required the use of both optical and electron microscopy. The presence and extent of the cellular precipitation could be observed most readily in optical micrographs (X100 or X1,000), and the existence of overaged γ' particles in the matrix could generally be deduced from the general darkening of the matrix in these micrographs. In order to observe the fine details of the size, shape, and distribution of the γ' particles and of the structure of the cellular precipitate, however, electron microscopy was required. Methods of preparing alloy specimens for observation by electron and optical microscopy have been described in the section "Experimental Procedures."

Attempts have been made to relate the observed microstructure to the hardness of the alloy and its stress-rupture properties measured at 1,600° F and 25,000 psi. Hardness generally appeared to be most closely related to the distribution of the γ' particles within the matrix of the alloy; that is, a fine dispersion of small particles was usually accompanied by high hardness while the overaged structures involving the large, widely separated particles were associated with lower hardness. However, microstructural observations are not completely effective in correlating all observed variations in hardness. The fact that aging specimens at 1,000° and 1,200° F after solution treatment at 2,150° F and ice-brine-quenching produced increases in hardness without producing detectable γ' particles is a case in point. It may be that here γ' particles were produced which were too fine to be resolved by the etching and replicating techniques used in obtaining the electron micrographs. A similar explanation may account for the fact that the alloy did not soften as much as might be expected upon solution treatment at 2,000° F and ice-brine-quenching, and that its hardness after this treatment was higher than after solution treatment at 1,900° F and ice-brine-quenching. In this case, however, solution hardening due to more complete dissolving of the elements forming the γ' phase may be involved.

The stress-rupture properties of the alloy appear to be more closely related to the conditions of the grain boundaries than to the general precipitation of the γ' phase within the matrix. It appears that overaged conditions at the grain-boundary regions are associated with weakness in the 1,600° F rupture tests. These conditions can develop from aging during testing or from treatments prior to the start of a rupture test, as was the case for ice-brine-quenching or furnace-cooling after solution treatment. Material treated only at 1,975° F was more prone to the development of this type of structure during testing than material heated at 2,150° F, apparently because the higher temperature is more effective in removing residual rolling effects. It is highly possible that the weakness and overaged grain-boundary structures are due to strain-induced phenomena arising from quenching stresses, residual cold work from rolling and, in rupture testing, from yielding and creep.

Since the alloy seemed to be sensitive to strain, the influence of rolling when solution treatments are carried out at about 1,975° F would be expected to be variable. If the rolling gave uniform complete recrystallization, it might have considerably less effect. Likewise, if enough residual strain was left to give uniform recrystallization on heating to 1,975° F, the rolling should have little effect. The restrictions imposed by the limited range of temperatures and reduction of hot-rolling needed to minimize cracking, however, suggest that this alloy should usually be improved by a higher temperature treatment. It is strongly suspected that the alloy is subject to considerable loss in strength at 1,600° F from small amounts of cold-work. Because the alloy apparently cold-works to a considerable extent during working at temperatures as high as 2,150° F, and since considerable time is needed to anneal the alloy even at 2,150° F, the chances are that there are only rare cases where the 2,150° F treatment would not be beneficial.

In conclusion, it is known that very small amounts of such elements as boron, zirconium, and possibly magnesium have very pronounced effects on strength and ductility in rupture tests (ref. 14). Work is in progress to determine how the presence of traces of such elements affect the microstructures and properties of this and similar alloys. Until such studies are complete and further verification of the relationships are obtained experimentally, it cannot be estimated to what extent the results described here can be extrapolated to other alloys and other conditions of heat treatment and testing. However, it can be noted that general trends in the variations of hardness and stress-rupture properties with heat treatment described for the experimental alloy used here are similar to those which have been observed in limited studies of other experimental alloys of similar compositions.

CONCLUSIONS

The study of effects of heat treatments on microstructures and high-temperature stress-rupture properties of a nickel-base alloy hardened with titanium and aluminum resulted in the following results and conclusions:

1. The solution temperature for complete solution of γ' and grain-boundary carbides during a 4-hour heat treatment was between 1,975° and 2,000° F.

2. Heat treatment at 1,800° to 1,900° F led to overaging of the alloy. The coarse general precipitate of γ' particles was obtained in this range and resulted in significantly lower hardness than that obtained in the completely solution-treated and quenched condition.

3. The rupture life of stock solution-treated 4 hours at 1,975° F and then air-cooled was inferior to that of stock treated 2 hours at 2,150° F and air-cooled. This was related to residual rolling effects which were not removed by the 1,975° F treatment.

4. Cooling rate after solution treatment markedly affected the precipitation reaction during the cooling period and during subsequent aging. Rapid general precipitation of γ' occurred during cooling. Considerable suppression of the reaction was obtained by ice-brine-quenching although it was not proved that suppression was complete. Precipitation increased inversely with cooling rate, air-cooling giving a general fine precipitate but furnace-cooling, a coarse overaged general precipitate. Aging of the ice-brine-quenched stock led to cellular precipitation at the grain boundaries.

5. Cooling rate after solution treatment also had a marked effect on high-temperature properties. Solution-treated, ice-brine-quenched, and aged stock ruptured upon loading at 1,600° F and 25,000 psi with negligible ductility. This conduct was related to the cellular precipitate. Furnace-cooling after solution treatment resulted in inferior rupture life when compared with air-cooling because the furnace-cooled sample was overaged before testing.

6. Isothermal-aging studies revealed that general precipitation of γ' particles proceeded at 1,200°, 1,400°, and 1,600° F. Localized precipitation of γ' particles and carbides appeared at grain boundaries at 1,400° and 1,600° F. No overaging was evident during 100 hours at 1,200° and 1,400° F, but overaging did occur after 4 hours at 1,600° F. No significant effect of the double-aging treatment after solution-treating and air-cooling on rupture life was found.

7. Comparison of samples rupture-tested at 1,600° F with those aged at 1,600° F without stress revealed that stress had little effect on the precipitation of the γ' particles within the alloy matrix. Stressing did appear to cause severe agglomeration and overaging to a greater extent at the grain boundaries. In addition, stressing prevented the dropoff of hardness that accompanied overaging of the matrix precipitate in the isothermally-aged unstressed samples.

It is concluded that effects of heat treatments on the high-temperature properties of the nickel-base alloy hardened with titanium and aluminum were related to the size and distribution of the γ' phase, provided that residual rolling effects were removed by the solution treatment, as follows:

(1) Treatments which provided a finely dispersed general precipitate of γ' with no overaged areas of depleted matrix resulted in essentially equal properties at 1,600° F and 25,000 psi.

(2) Treatments such as ice-brine-quenching or furnace-cooling which resulted in overaging of portions of the stock (the cellular precipitate in the case of ice-brine-quenching and the general precipitate in the case of furnace-cooling) lowered the high-temperature life.

University of Michigan,
Ann Arbor, Mich., January 30, 1957.

APPENDIX

ANALYSIS OF SIGNIFICANCE OF PROPERTY DIFFERENCES

Data from 45 hardness impressions and 50 rupture tests were analyzed to estimate testing scatter. The purpose of this analysis was to determine if property differences obtained in the investigation were significant or if they could be accounted for by testing scatter alone. The symbols used in the discussion of the analysis are as follows:

N	number of tests on each sample
s	$(\text{variance of test results})^{1/2}$
t	value from table B of reference 15 using one tail test and 95-percent confidence limit, given by equation (2)
X	test result
$\bar{X}$	average of test results

Subscripts:

1,2	samples 1 and 2, respectively

The data were analyzed to establish the variance of test results s^2 by using the following formula from the work of Duncan (ref. 15):

$$s^2 = \frac{\sum (X - \bar{X})^2}{N - 1} \tag{1}$$

Once s^2 had been established for the testing method for hardness or rupture life, the significance of differences in hardness or rupture times could be estimated using the difference test and the t distribution table of Duncan (ref. 15):

$$t = \frac{\bar{X}_1 - \bar{X}_2}{s\sqrt{\frac{1}{N_1} + \frac{1}{N_2}}} \tag{2}$$

Hardness

Forty-five hardness impressions with two diagonal measurements per impression were used to calculate

$$s^2 = 9.65 \tag{3}$$

for a single diagonal measurement in ocular reading units.

Using the t distribution, the average diagonal measurement difference which was required for 95-percent confidence of a true hardness difference was

$$\bar{X}_1 - \bar{X}_2 = t\left(s\sqrt{\frac{1}{N_1} + \frac{1}{N_2}}\right) \tag{4}$$

With $N_1 = N_2 = 6$,

$$\bar{X}_1 - \bar{X}_2 = (1.67)(1.79)$$

$$= 2.99$$

In the range of 300 to 340 VPN, 1 unit of ocular reading equals 2.35 VPN. Therefore, the difference in VPN between two specimens needed for 95-percent confidence of a true hardness difference was

$$(2.99)(2.35) = 7 \text{ VPN} \tag{5}$$

In the range of 340 to 400 VPN, 1 unit of ocular reading equals 3 VPN. Therefore, the difference in VPN between two specimens needed for 95-percent confidence of a true hardness difference was

$$(2.99)(3) = 9 \text{ VPN} \tag{6}$$

Therefore, when a greater difference than this was observed between the hardness of any two samples, the difference was considered significant.

Rupture Life

Fifty stress-rupture tests were run at 1,600° F and 25,000 psi. Two tests were run on each of 23 experimental heats of a 55Ni-20Cr-15Co-4Mo-3Ti-3Al alloy and four tests were run on another heat. The average rupture life of these heats varied from 48.3 hours to 646.1 hours. The analysis yielded

$$s^2 = 0.00298 \tag{7}$$

as the variance of the logarithm of the rupture life (in hours) of a rupture test.

Assuming that s^2 does not vary with rupture life and using the t distribution, the difference of the logarithm of rupture life which is required for 95-percent confidence of true strength difference was

$$\bar{X}_1 - \bar{X}_2 = t\left(s\sqrt{\frac{1}{N_1} + \frac{1}{N_2}}\right) \tag{8}$$

With $N_1 = 2$ and $N_2 = 2$,

$$\bar{X}_1 - \bar{X}_2 = (1.706)(0.0545)$$

$$= 0.093$$

Therefore, a difference of 0.093 in the logarithm of rupture life between two conditions can be considered significant when $N_1 = 2$ and $N_2 = 2$.

This result has been applied to figure 4 by placing limits around the average rupture life for treatment B (2 hours at 2,150° F, then air-cooled). The limits were calculated as 113 to 174 hours. When the average rupture life of two tests with another heat treatment fell outside these limits, this treatment was considered to give a significant change in high-temperature life from the life obtained with treatment B.

Heat treatments A and F in figure 4 (see table II for key to heat-treatment designations) were, therefore, considered to give inferior

high-temperature life. Only one rupture test was needed for treatment D to show its obvious inferiority. However, the rupture lives of the samples used in the single tests run with treatments C, E, and G were so close to that of the sample with treatment B that additional tests were not needed to show further the comparability of their rupture properties.

REFERENCES

1. Nordheim, R., and Grant, N. J.: Aging Characteristics of Nickel-Chromium Alloys Hardened With Titanium and Aluminum. Jour. Metals, vol. 6, no. 2, sec. 2 (Trans.), Feb. 1954, pp. 211-218.

2. Taylor, A.: Constitution of Nickel-Rich Quaternary Alloys of the Ni-Cr-Ti-Al System. Jour. Metals, vol. 9, no. 1, sec. 2 (Trans.), Jan. 1957, pp. 71-75.

3. Betteridge, W., and Franklin, A. W.: Les progrès des alliages à base de nickel-chrome en service à haute temperature. Rev. métallurgie, t. 53, pt. 4, Apr. 1956, pp. 271-284.

4. Freeman, James Wright, and Corey, C. L.: Microstructure and Creep. Symposium on Creep and Fracture of Metals at High-Temperatures (May 31 - June 2, 1954), Nat. Phys. Lab. (London), 1956, pp. 157-173.

5. Frey, D. N., Freeman, J. W., and White, A. E.: Fundamental Aging Effects Influencing High-Temperature Properties of Solution-Treated Inconel X. NACA TN 2385, 1951.

6. Brockway, L. O., and Bigelow, W. C.: The Investigation of the Minor Phases of Heat-Resistant Alloys by Electron Diffraction and Electron Microscopy. WADC TR 54-589, Contract AF-33(616)-23, WADC and Univ. of Mich., May 1955.

7. Betteridge, W., and Smith, R. A.: Effect of Heat Treatment and Structure Upon Creep Properties of Nimonic Alloys Between 750 and 950° C. Symposium on Metallic Materials for Service at Temperatures Above 1600° F. Special Tech. Pub. No. 174, ASTM, 1956.

8. Geisler, A. H.: Precipitation from Solid Solutions of Metals. Phase Transformations in Solids, R. Smoluchowski, ed., John Wiley & Sons, Inc., 1951, pp. 387-544.

9. Bigelow, W. C., Amy, J. A., and Brockway, L. O.: A Selective Etching Procedure for Identifying the γ' Phase of Nickel-Base Alloys by Electron Microscopy. Proc. ASTM, vol. 56, pp. 945-953.

10. Dennison, J. P.: Some Creep Characteristics of a Group of Precipitation-Hardening Alloys Based on the Alpha-Copper-Aluminum Phase. The Jour. Inst. Metals, vol. 82, pt. 3, Nov. 1953, pp. 117-128.

11. Roberts, C. S.: Interaction of Precipitation and Creep in Mg-Al Alloys. Jour. Metals, vol. 8, no. 2, sec. 2 (Trans.), Feb. 1956, pp. 146-148.

12. Baillie, Y., and Poulignier, J.: Etude la précipitation submicroscopique dans les alliages refractaires nickel-chrome. Rev. métallurgie, t. 51, pt. 3, Mar. 1954, pp. 179-191.

13. Decker, R. F., Rush, A. I., Dano, A. G., and Freeman, J. W.: Abnormal Grain Growth in Nickel-Base Heat-Resistant Alloys. NACA TN 4082, 1956.

14. Decker, R. F., Rowe, J. P., and Freeman, J. W.: Influence of Crucible Materials on the High-Temperature Properties of a Vacuum-Melted Nickel-Chromium-Cobalt Alloy. NACA TN 4049, 1957.

15. Duncan A. J.: Quality Control and Industrial Statistics. Richard D. Irwin, Inc. (Homewood, Ill.), 1952.

TABLE I

ETCHANTS USED IN METALLOGRAPHIC STUDY

Designation	Composition	
	Component	Percent by volume
Etchant A	Cupric chloride solution[a]	29
	Acetic acid (glacial)	36
	Hydrochloric acid (38 percent)	23
	Sulfuric acid (96 percent)	5
	Chromic acid[b]	7
Etchant B	Phosphoric acid (85 percent)	12
	Sulphuric acid (96 percent)	47
	Nitric acid (70 percent)	41
Etchant C	Phosphoric acid (85 percent)	11
	Sulphuric acid (96 percent)	45
	Nitric acid (70 percent)	29
	Water	15
Etchant D	Sulphuric acid (96 percent)	21
	Hydrochloric acid (38 percent)	15
	Nitric acid (70 percent)	21
	Hydrofluoric acid (48 percent)	21
	Water	22
Etchant E	Cupric chloride solution[a]	40
	Hydrochloric acid (38 percent)	40
	Hydrofluoric acid (48 percent)	20

[a]Solution of 1 g $CuCl_2 \cdot 2H_2O$ per 5 ml of H_2O.

[b]Solution of 1 g CrO_3 per 3 ml of H_2O.

TABLE II

STRESS-RUPTURE DATA FOR SPECIMENS TESTED AT 1,600° F AND 25,000 PSI

Treatment designation	Solution treatment			Aging treatment			Figure showing microstructure		Rupture, time, hr	Elongation, percent	Reduction of area, percent	Hardness, VPN	
	Time, hr	Temperature, °F	Cooling medium	Time, hr	Temperature, °F	Cooling medium	Before testing	After testing				Before testing	After testing
A	4	1,975	Air	———	———	—	3(a)	8	71.7 48.7	7 15	8 12	380	368
B	2	2,150	Air	———	———	—	3(b)	9	147.4 133.7	5 6	5 8	353	365
C	2 Plus 4	2,150 1,975	Air Air	———	———	—	3(c)	—	138.1	4	5	354	362
D	2 Plus 4	2,150 1,975	Ice-brine Ice-brine	24 Plus 16	1,550 1,400	Air Air	3(d)	11	Broke on loading	<1	<1	402	402
E	2 Plus 4	2,150 1,975	Air Air	24 Plus 16	1,550 1,400	Air Air	3(e)	12	152.9	3	6	380	362
F	2	2,150	Furnace	———	———	—	3(f)	13	77.3 69.6	9 6	8 7	311	325
G	2	2,150	Air	24 Plus 16	1,550 1,400	Air Air	3(g)	—	127.6	5	3	389	362

TABLE III

HARDNESS DATA

[Vickers penetration hardness measured with 50,000 gram load]

Original condition	Solution treatment			Aging treatment			Hardness, VPN
	Time, hr	Temperature, °F	Cooling medium	Time, hr	Temperature, °F	Cooling medium	
As cast (ingot center)	------	-----	---------	-------	-----	---------	335
As cast (ingot surface)	------	-----	---------	-------	-----	---------	325
As rolled	------	-----	---------	-------	-----	---------	362
As rolled	4	1,975	Air	-------	-----	---------	380
As rolled	2	2,150	Air	-------	-----	---------	356, 354, 349
As rolled	2	2,150	Furnace	-------	-----	---------	311
As rolled	2	2,150	Air	-------	-----	---------	354
	Plus 4	1,975	Air				
As rolled	2	2,150	Air	24	1,550	Air	380
	Plus 4	1,975	Air	Plus 16	1,400	Air	
As rolled	2	2,150	Ice-brine	24	1,550	Air	402
	Plus 4	1,975	Ice-brine	Plus 16	1,400	Air	
As rolled	2	2,150	Air	24	1,550	Air	389
				Plus 16	1,400	Air	
As rolled	2	2,150	Air	4	1,700	Ice-brine	348
As rolled	2	2,150	Air	4	1,800	Ice-brine	298
As rolled	2	2,150	Air	4	1,900	Ice-brine	276
As rolled	2	2,150	Air	4	2,000	Ice-brine	306
As rolled	2	2,150	Ice-brine	-------	-----	---------	313
As rolled	2	2,150	Water	-------	-----	---------	324
As rolled	2	2,150	Ice-brine	1	1,000	Air	333
As rolled	2	2,150	Ice-brine	10	1,000	Air	328
As rolled	2	2,150	Ice-brine	100	1,000	Air	340
As rolled	2	2,150	Ice-brine	1	1,200	Air	345
As rolled	2	2,150	Ice-brine	10	1,200	Air	357
As rolled	2	2,150	Ice-brine	100	1,200	Air	374
As rolled	2	2,150	Ice-brine	1	1,400	Air	345
As rolled	2	2,150	Ice-brine	10	1,400	Air	380
As rolled	2	2,150	Ice-brine	100	1,400	Air	398
As rolled	2	2,150	Ice-brine	1	1,600	Air	365
As rolled	2	2,150	Ice-brine	4	1,600	Air	389
As rolled	2	2,150	Ice-brine	10	1,600	Air	365
As rolled	2	2,150	Ice-brine	100	1,600	Air	345
As rolled	2	2,150	Air	1	1,000	Air	345
As rolled	2	2,150	Air	10	1,000	Air	357
As rolled	2	2,150	Air	100	1,000	Air	362
As rolled	2	2,150	Air	1	1,200	Air	359
As rolled	2	2,150	Air	10	1,200	Air	368
As rolled	2	2,150	Air	100	1,200	Air	383
As rolled	2	2,150	Air	1	1,400	Air	377
As rolled	2	2,150	Air	10	1,400	Air	383
As rolled	2	2,150	Air	100	1,400	Air	392
As rolled	2	2,150	Air	1	1,600	Air	359
As rolled	2	2,150	Air	4	1,600	Air	374
As rolled	2	2,150	Air	10	1,600	Air	354
As rolled	2	2,150	Air	100	1,600	Air	328

TABLE IV

X-RAY DIFFRACTION DATA

[Solid samples, unfiltered K radiation, chromium target]

Miller indices, (hkl)	4 hr at 1,900° F, ice-brine-quenched				4 hr at 2,000° F, ice-brine-quenched			
	Distance between planes, A	Estimated intensity		Possible phase	Distance between planes, A	Estimated intensity		Possible phase
		K_α	K_β			K_α	K_β	
100	3.56	Weak	Very weak	γ'	----	----------	------	-
110	2.52	Weak	---------	γ'	----	----------	------	-
111	2.06	Very strong	Strong	γ	2.07	Very strong	Strong	γ
200	1.79	Very strong	Strong	γ	1.79	Very strong	Strong	γ
220	1.27	Very strong	Strong	γ	1.27	Very strong	Medium	γ
300	1.19	Very weak	---------	γ'	----	----------	------	-
311	1.08	----------	Strong	γ	1.08	----------	Strong	γ

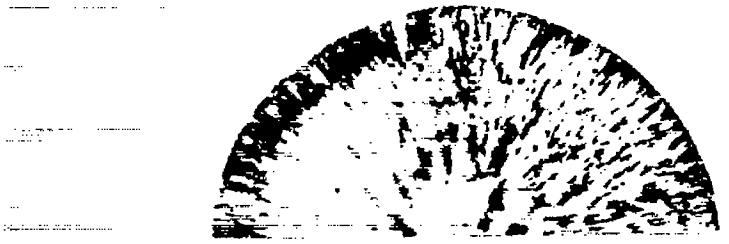

(a) Actual-size as-cast macrostructure of ingot section.

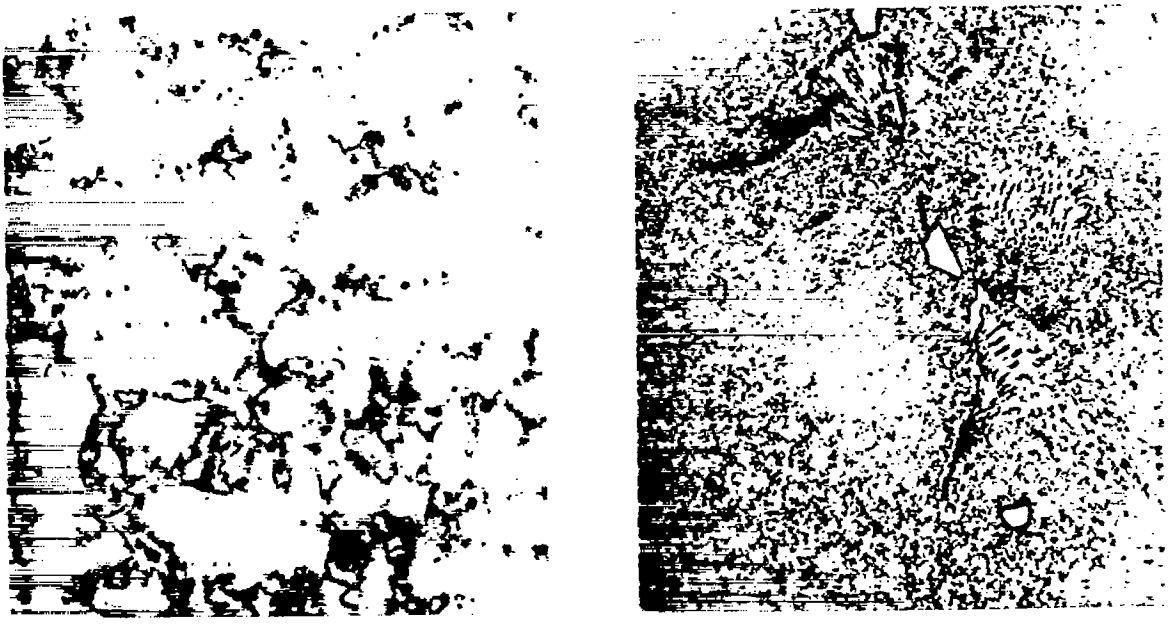

X100 X1,000

(b) As-cast microstructure at ingot center.

Figure 1.- As-cast structure of experimental alloy.

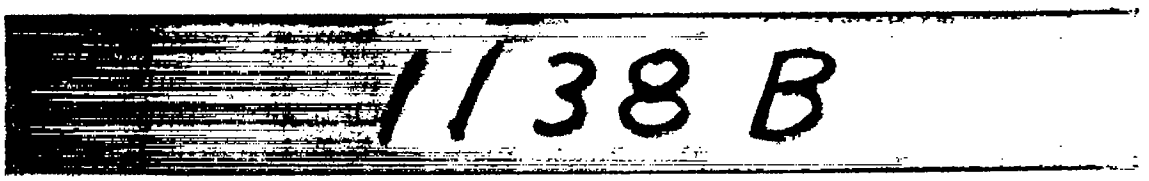

(a) As-rolled 7/8-inch bar stock.

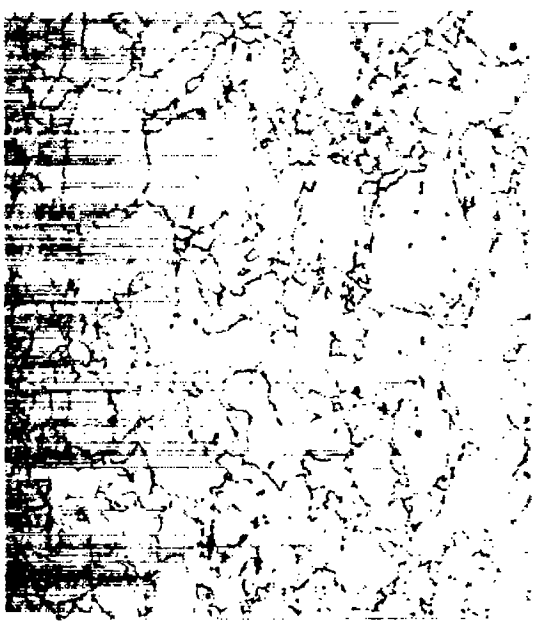

(b) As-rolled microstructure. Magnification, X100.

Figure 2.- As-rolled experimental alloy.

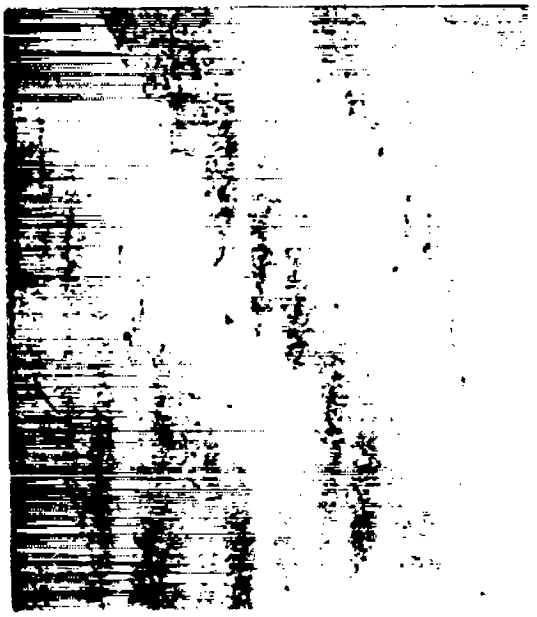

X100

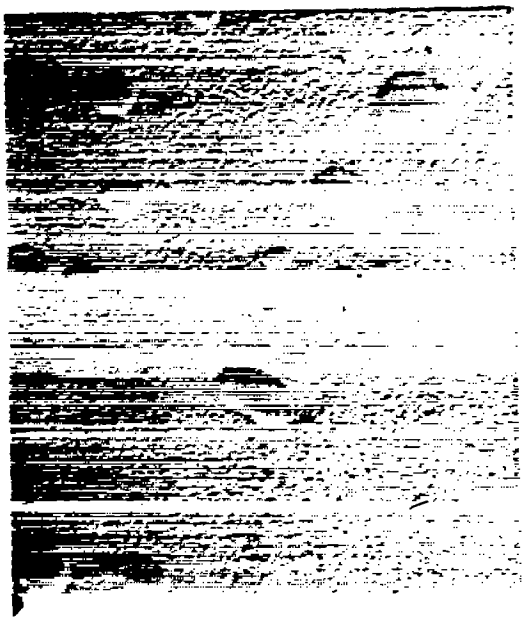

X13,000

(a) Treated 4 hours at 1,975° F, air-cooled; hardness, 380 VPN; average rupture life, 60 hours.

X100

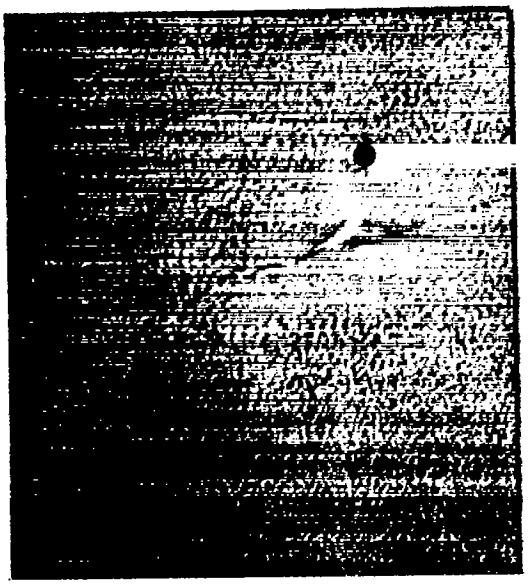

X13,000

(b) Treated 2 hours at 2,150° F, air-cooled; hardness, 353 VPN; average rupture life, 140 hours.

Figure 3.- Microstructures of alloy after heat treatment prior to rupture-testing at 1,600° F and 25,000 psi. Micrographs at X100 are optical micrographs; those at X13,000 are electron micrographs.

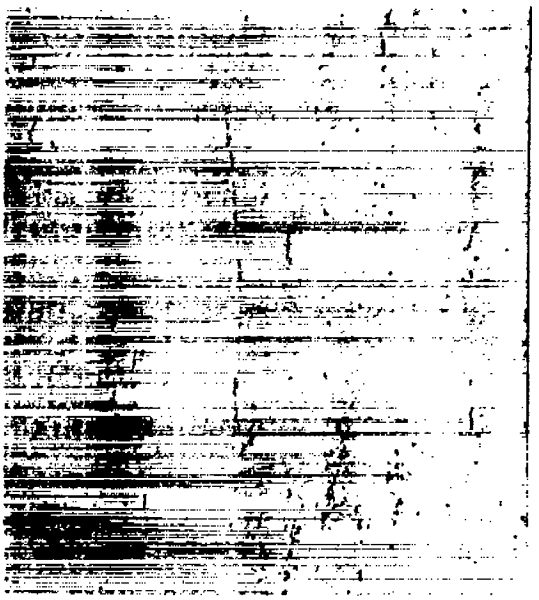

X100

X13,000

(c) Treated 2 hours at 2,150° F, air-cooled, plus 4 hours at 1,975° F, air-cooled; hardness, 354 VPN; rupture life, 138.1 hours.

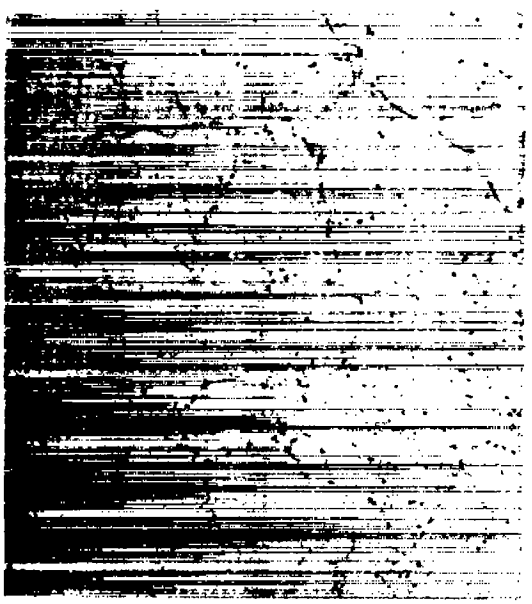

X100

X13,000

(d) Treated 2 hours at 2,150° F, ice-brine-quenched; plus 4 hours at 1,975° F, ice-brine-quenched, plus 24 hours at 1,550° F, air-cooled, plus 16 hours at 1,400° F, air-cooled; hardness, 402 VPN; rupture life, 0 hour (specimen broke on loading).

Figure 3.- Continued.

X100

X13,000

(e) Treated 2 hours at 2,150° F, air-cooled, plus 4 hours at 1,975° F, air-cooled, plus 24 hours at 1,550° F, air-cooled, plus 16 hours at 1,400° F, air-cooled; hardness, 380 VPN; rupture life, 152.9 hours.

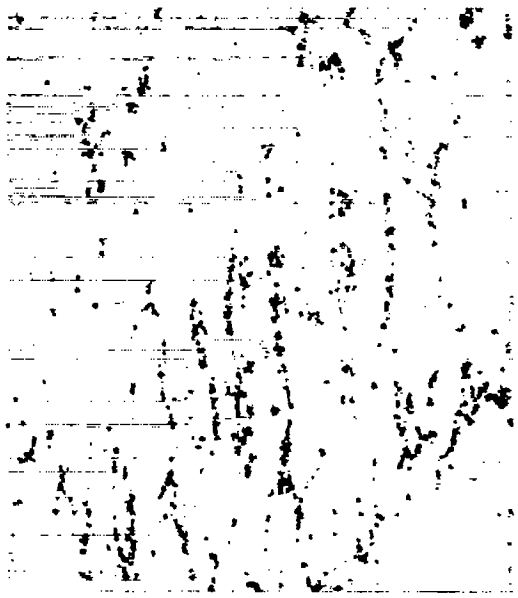

X100

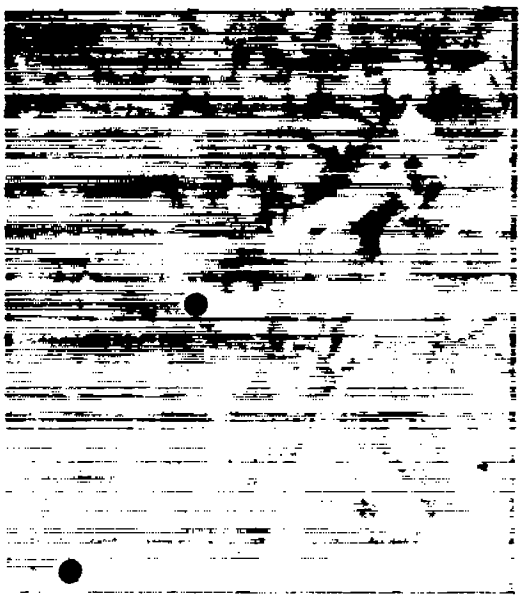

X13,000

(f) Treated 2 hours at 2,150° F, furnace-cooled; hardness, 311 VPN; average rupture life, 73 hours.

Figure 3.- Continued.

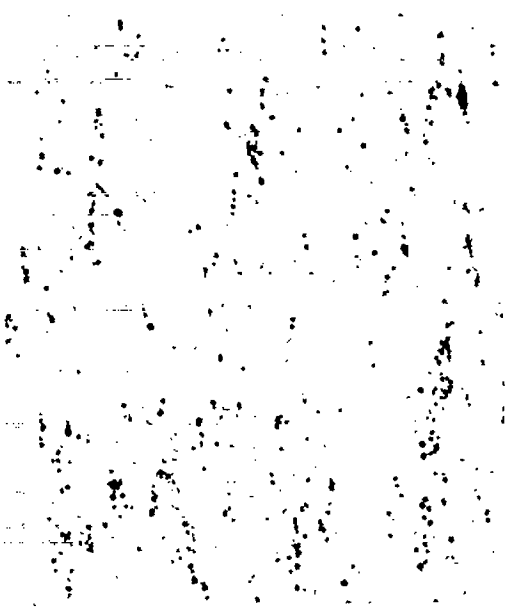

X100

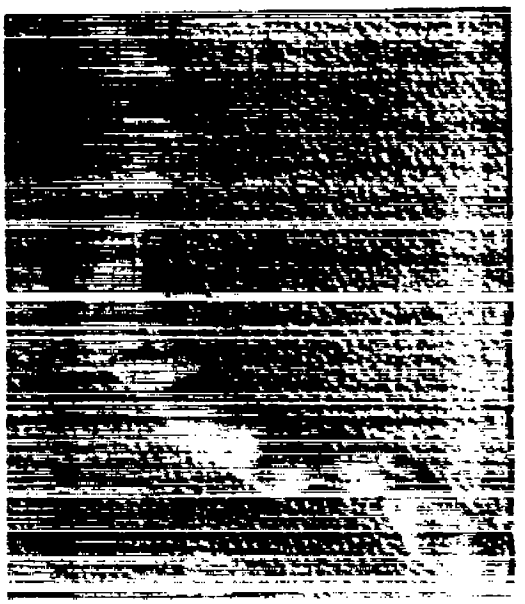

X13,000

(g) Treated 2 hours at 2,150° F, air-cooled, plus 24 hours at 1,550° F, air-cooled, plus 16 hours at 1,400° F, air-cooled; hardness, 389 VPN; rupture life, 127.6 hours.

Figure 3.- Concluded.

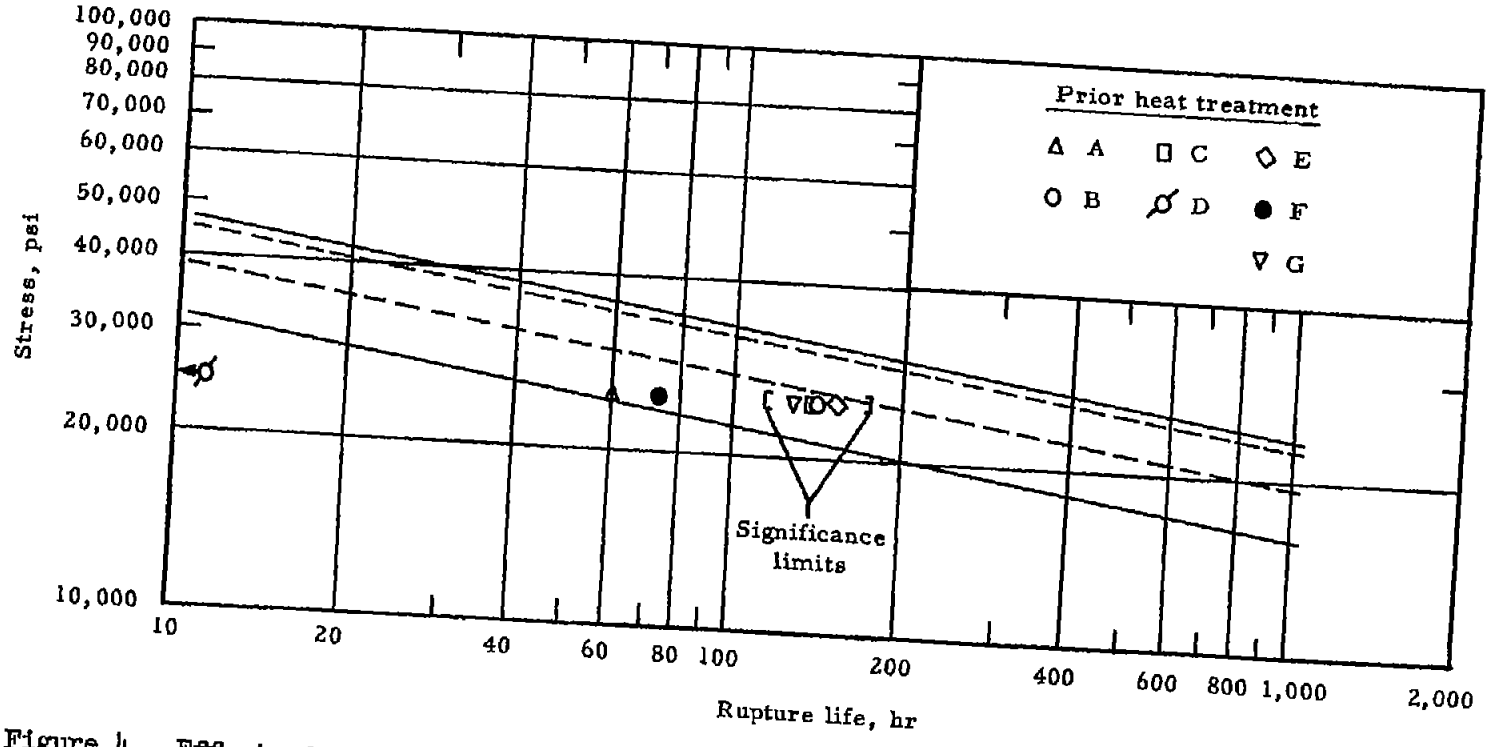

Figure 4.- Effect of prior heat treatment on rupture life at 1,600° F and 25,000 psi. Results are plotted on stress-rupture band for 55Ni-20Cr-15Co-4Mo-3Ti-3Al alloy. Dashed band is based on data on two heats of vacuum-melted Udimet 500 with treatment E reported by Utica Drop Forge and Tool Co. Solid band is extrapolated from data on vacuum-melted heats with treatment B processed at University of Michigan in study of effect of melting practice and chemistry on rupture life (ref. 13). See appendix for meaning of significance limits; see table II for key to heat treatments.

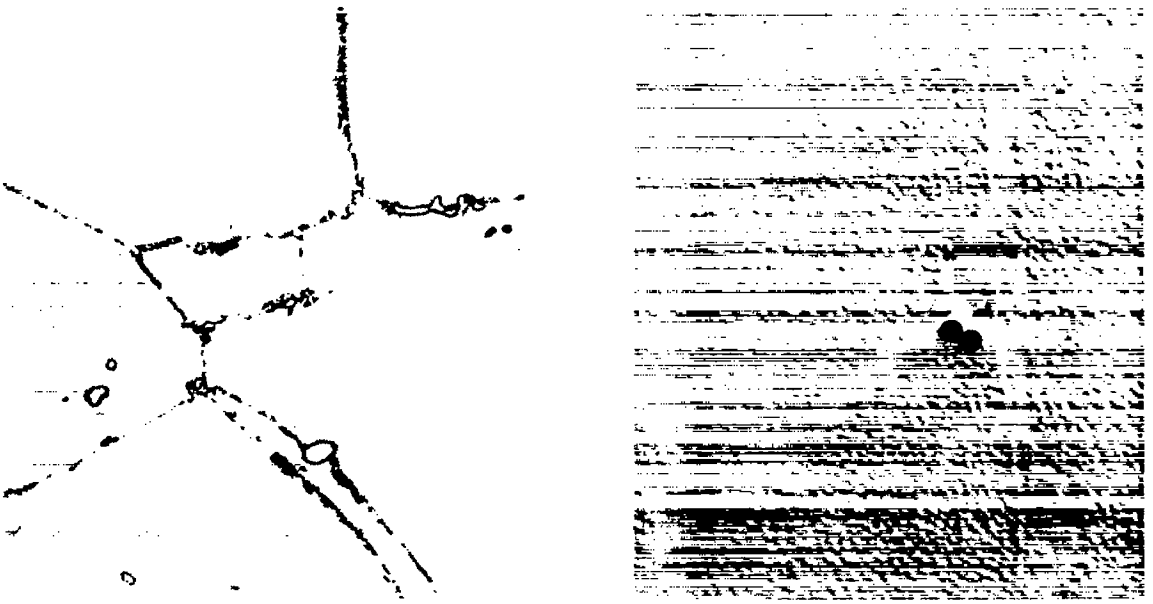

X1,000 X13,000

(a) 1,700° F, ice-brine-quenched; hardness, 348 VPN.

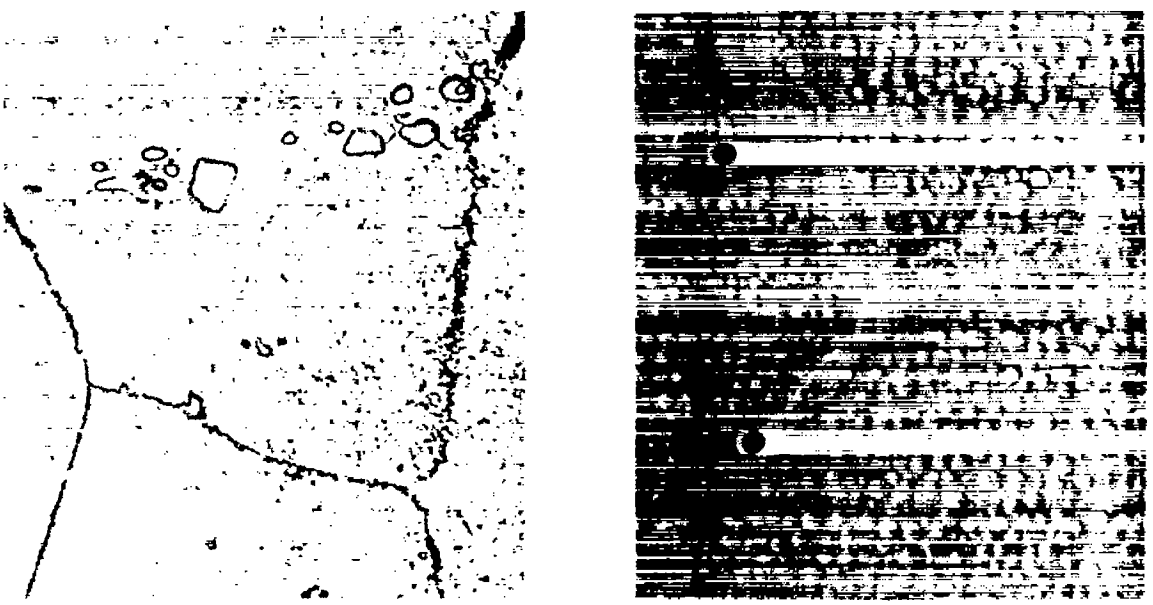

X1,000 X13,000

(b) 1,800° F, ice-brine-quenched; hardness, 298 VPN.

Figure 5.- Effect of 4-hour heat treatments at designated temperatures on microstructure. Rolled bar stock was treated 2 hours at 2,150° F, then air-cooled prior to heat treatment. Micrographs at X1,000 are optical micrographs; those at X13,000 are electron micrographs.

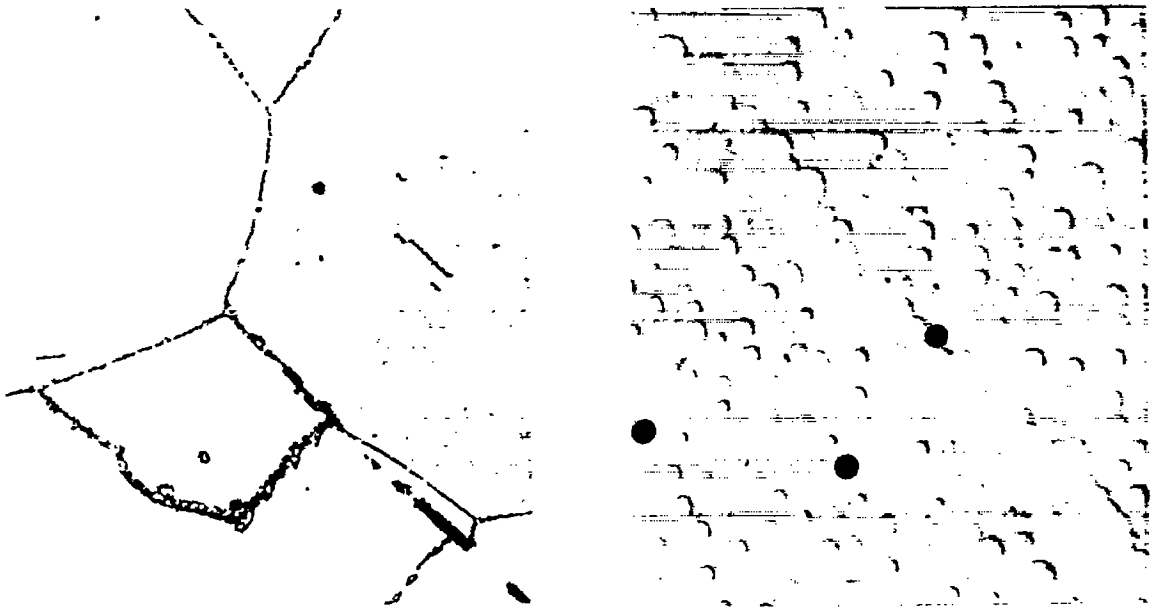

X1,000 X13,000

(c) 1,900° F, ice-brine-quenched; hardness, 276 VPN.

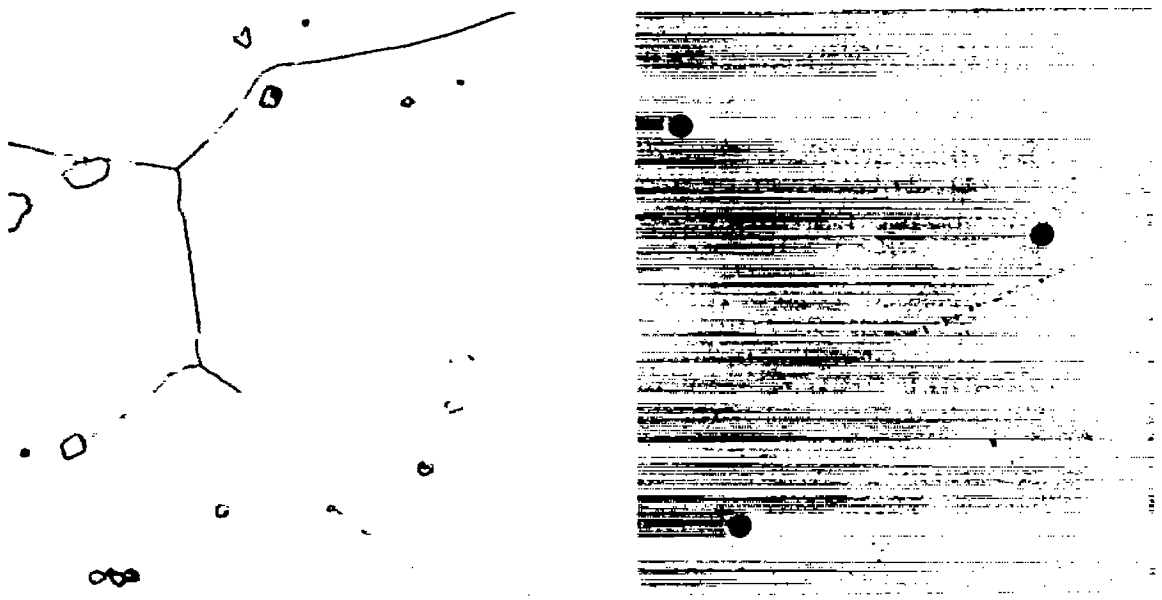

X1,000 X13,000

(d) 2,000° F, ice-brine-quenched; hardness, 306 VPN.

Figure 5.- Concluded.

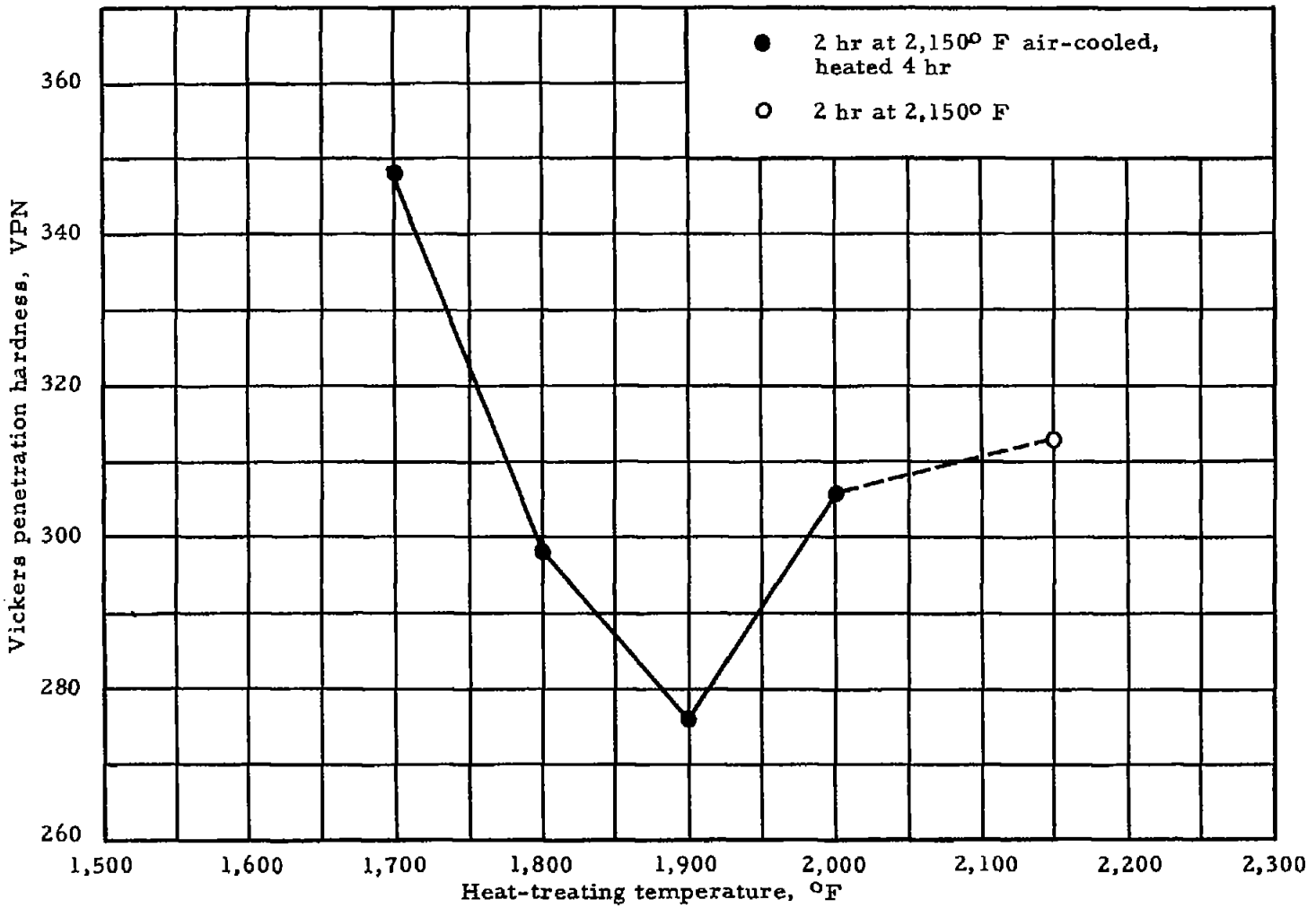

Figure 6.- Effect of heat-treating temperature on hardness. Samples were ice-brine-quenched after heat treatment.

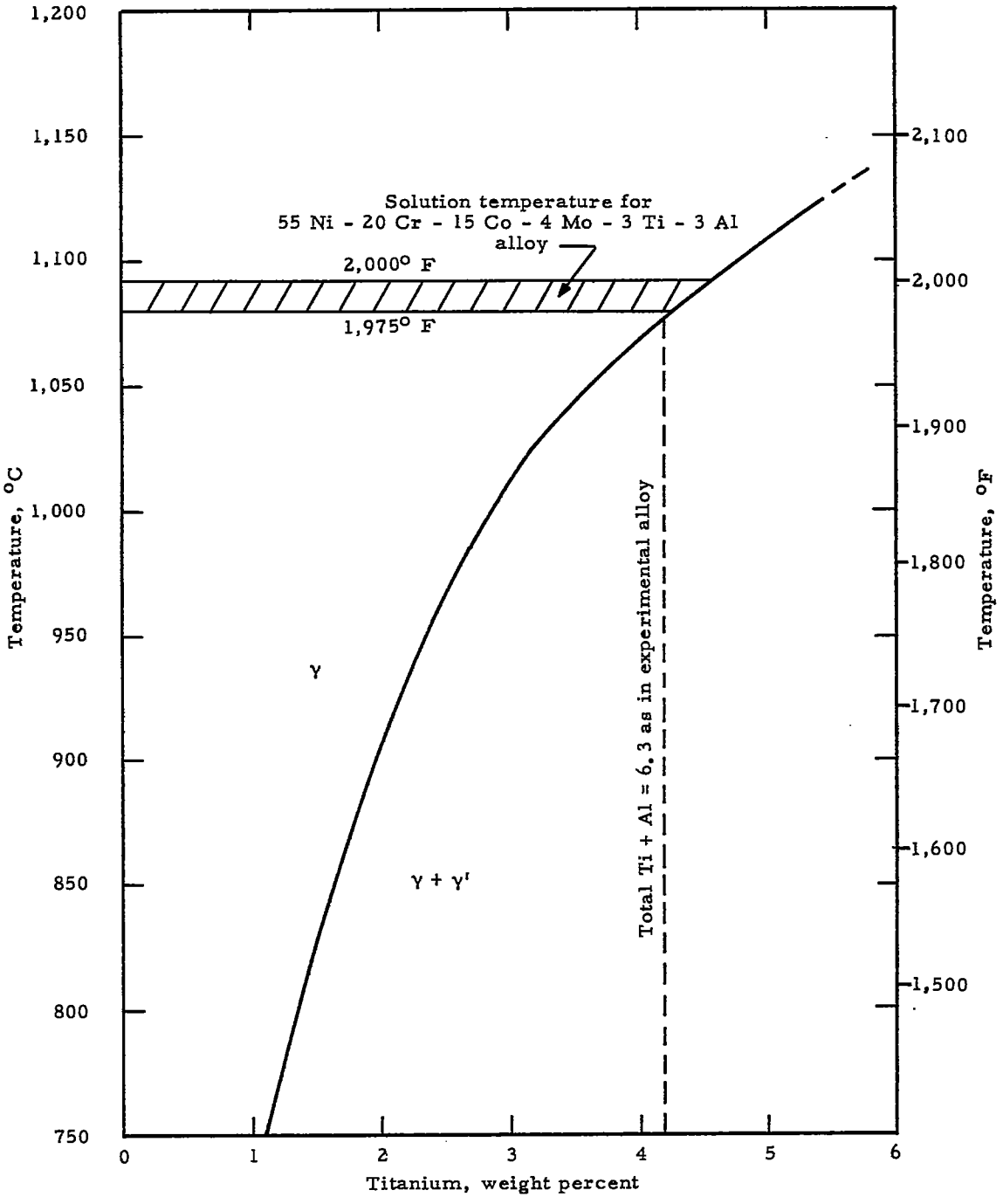

Figure 7.- Solution temperature of experimental 55Ni-20Cr-15Co-4Mo-3Ti-3Al alloy plotted on data of Betteridge and Franklin (ref. 3). Curve is for 60Ni-20Cr-20Co alloy with 2-to-1 ratio of titaniun to aluminum.

X100

X1,000

(a) Optical micrographs near fracture.

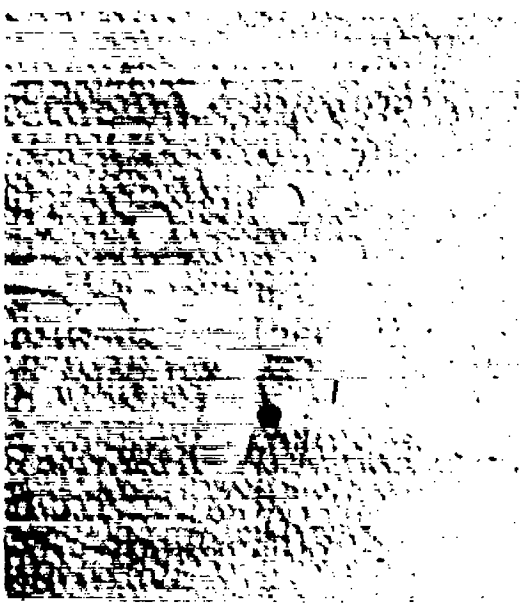

X13,000

(b) Electron micrograph of lightly agglomerated grain boundary.

X13,000

(c) Electron micrograph of heavily agglomerated grain boundary.

Figure 8.- Microstructure after rupture-testing at 1,600° F and 25,000 psi when prior heat treatment was 4 hours at 1,975° F, then air-cooled; hardness, 368 VPN; average rupture life, 60 hours.

X100

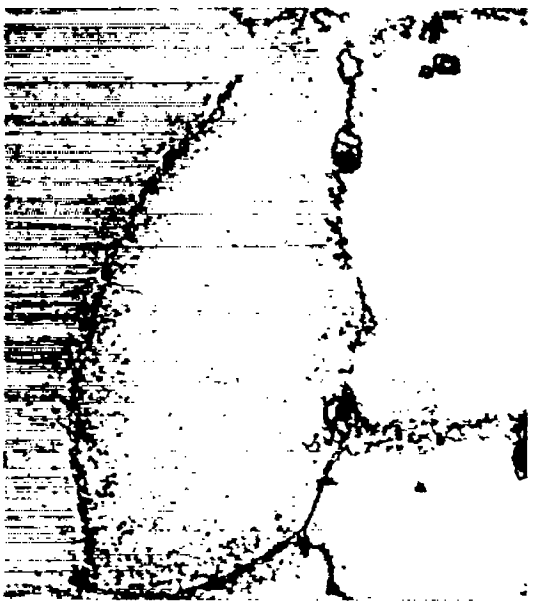

X1,000

(a) Optical micrograph near fracture.

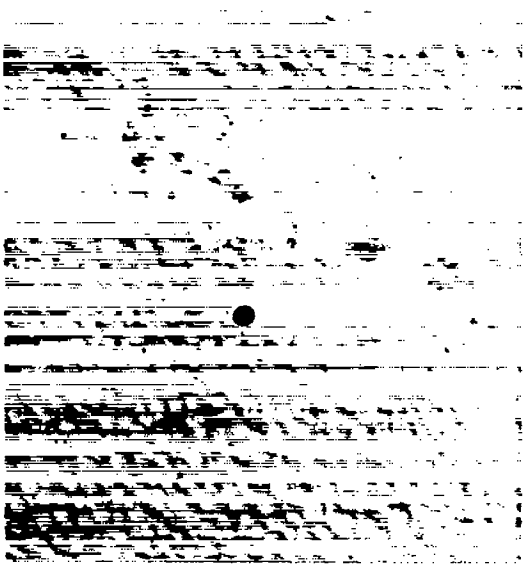

X13,000

(b) Electron micrograph of lightly agglomerated grain boundary.

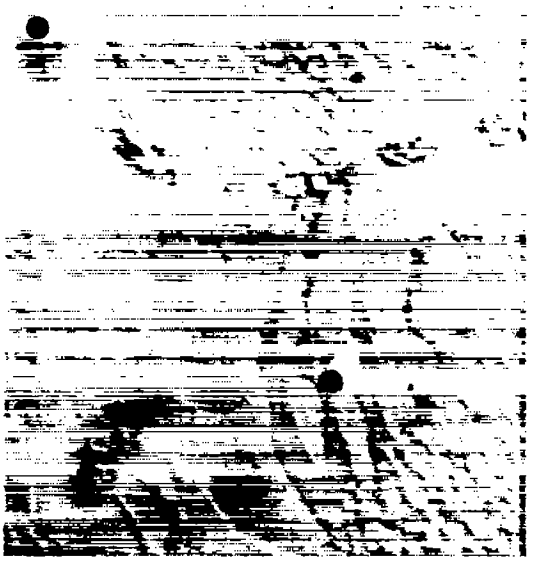

X13,000

(c) Electron micrograph of heavily agglomerated grain boundary.

Figure 9.- Microstructure after rupture-testing at 1,600° F and 25,000 psi when prior heat treatment was 2 hours at 2,150° F, then air-cooled; hardness, 365 VPN; average rupture life, 140 hours.

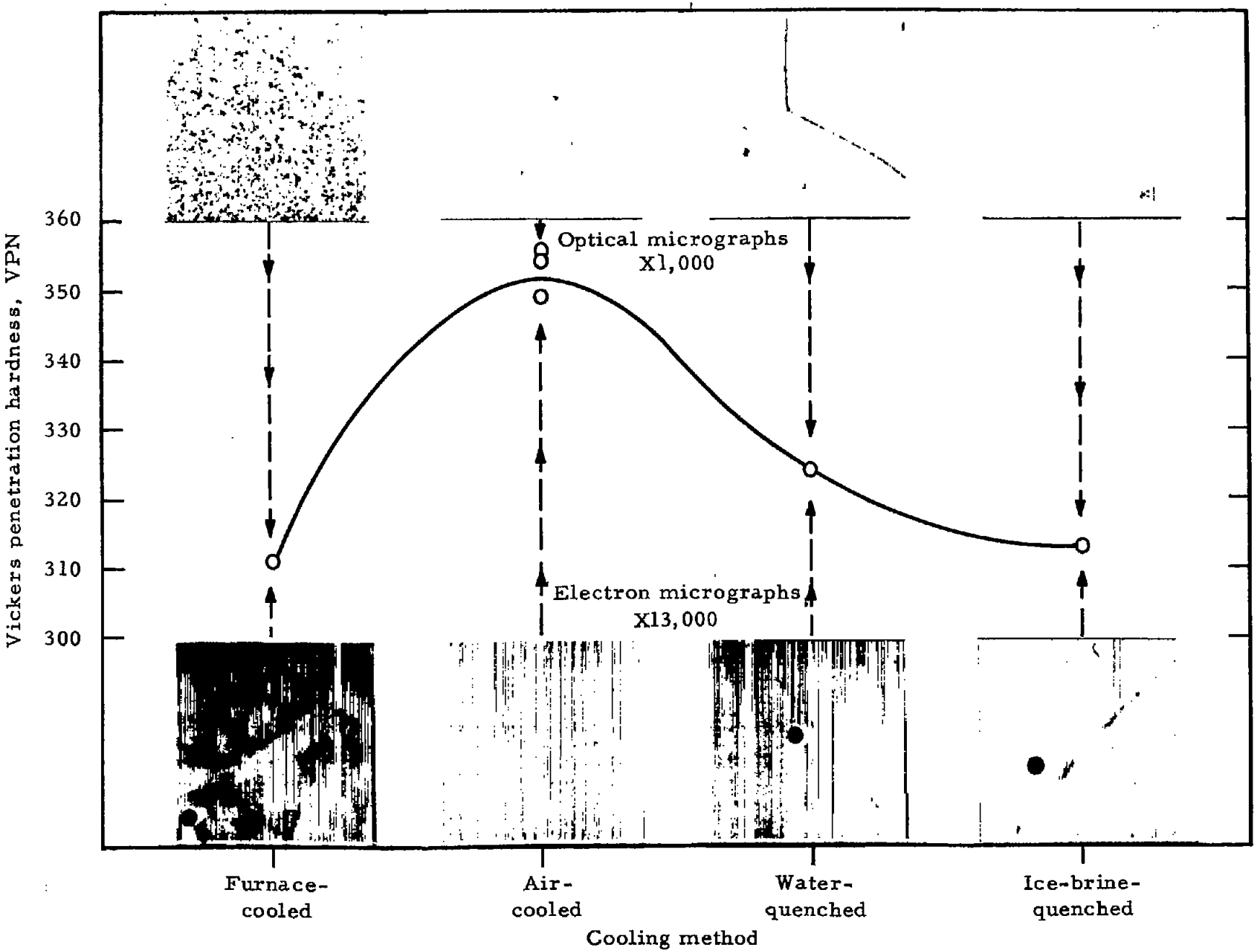

Figure 10.- Effect of cooling method after heat treatment of 2 hours at 2,150° F upon hardness and microstructure.

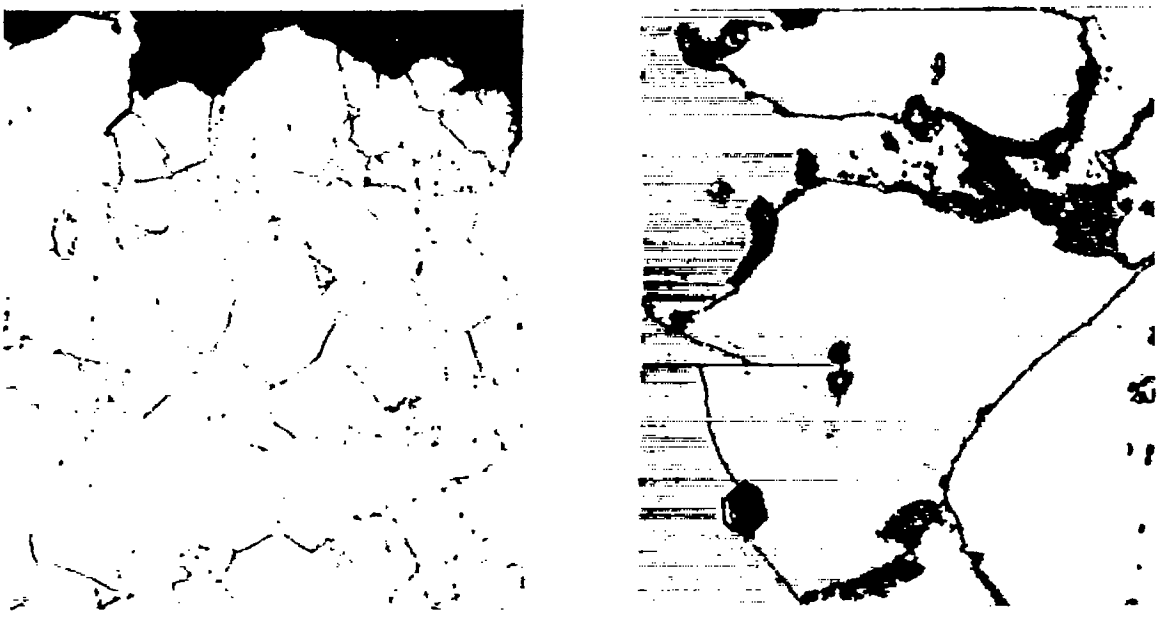

X100 X1,000

(a) Optical micrograph near fracture.

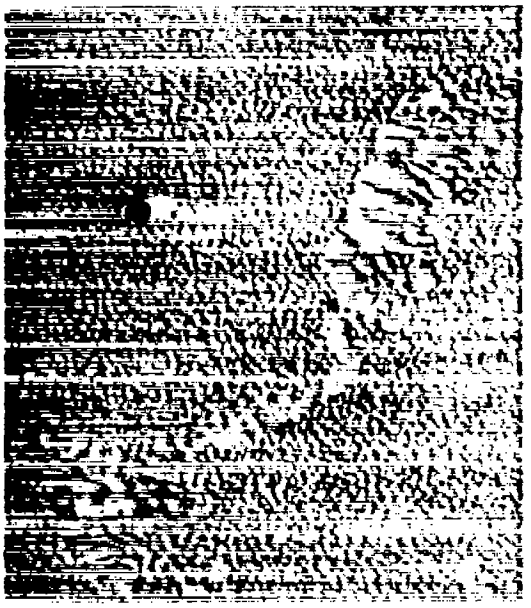

X13,000

(b) Electron micrograph.

Figure 11.- Microstructure after rupture-testing at 1,600° F and 25,000 psi when prior treatment was 2 hours at 2,150° F, ice-brine-quenched, plus 4 hours at 1,975° F, ice-brine-quenched, plus 24 hours at 1,550° F, air-cooled, plus 16 hours at 1,400° F, air-cooled; hardness, 402 VPN; rupture lift, 0 hour (broke on loading).

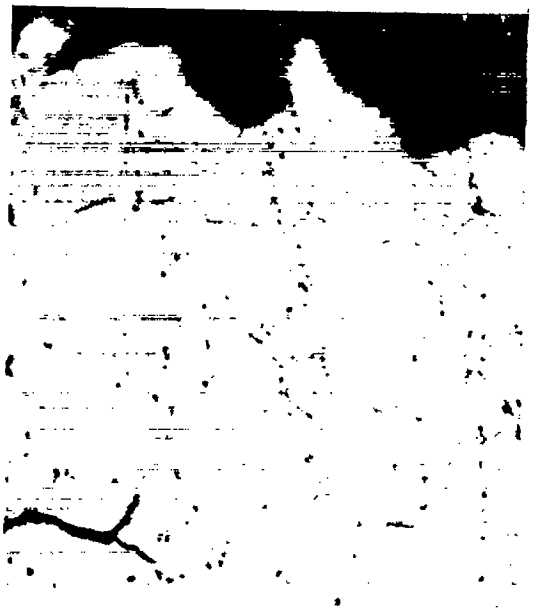

X100

X1,000

(a) Optical micrograph near fracture.

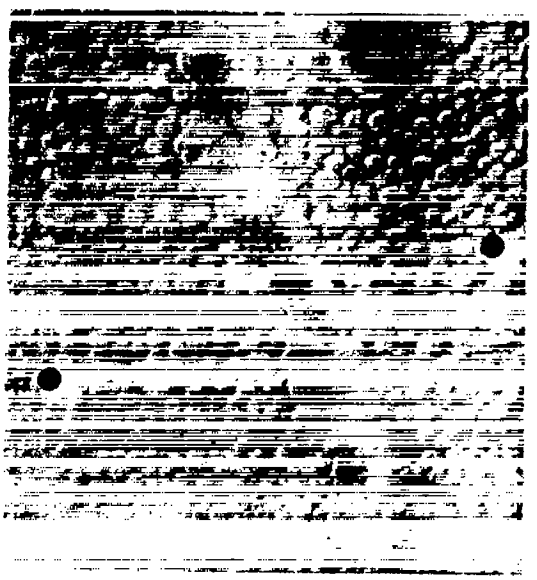

X13,000

(b) Electron micrograph of lightly agglomerated grain boundary.

Figure 12.- Microstructure after rupture-testing at 1,600° F and 25,000 psi when prior treatment was 2 hours at 2,150° F, air-cooled, plus 4 hours at 1,975° F, air-cooled, plus 24 hours at 1,550° F, air-cooled, plus 16 hours at 1,400° F, air-cooled; hardness, 362 VPN; rupture life, 152.9 hours.

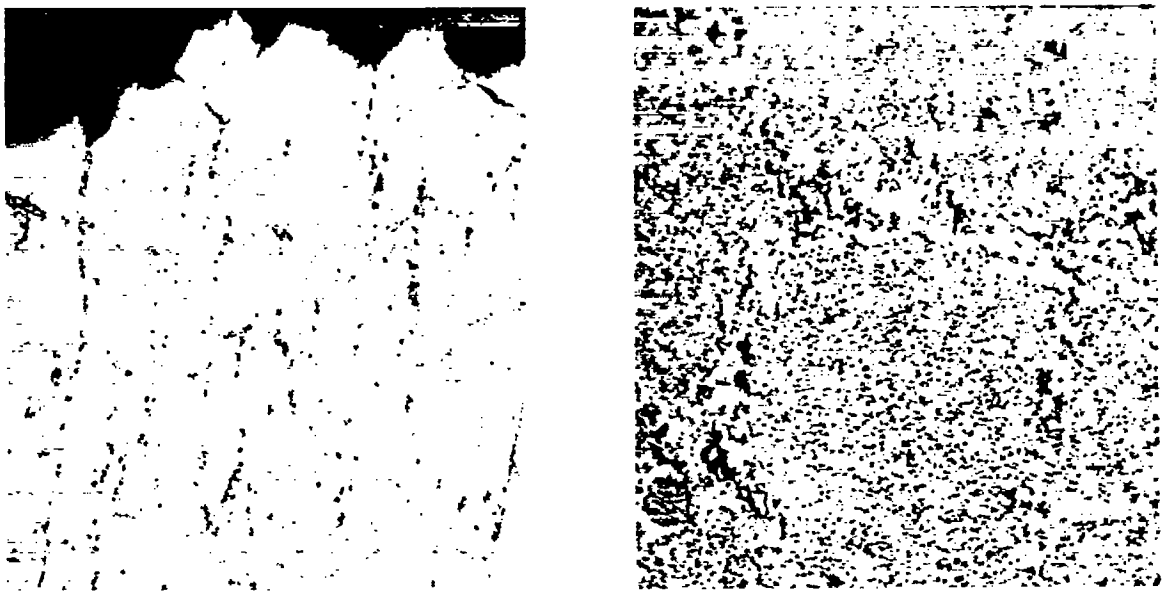

X100 X1,000

(a) Optical micrograph near fracture.

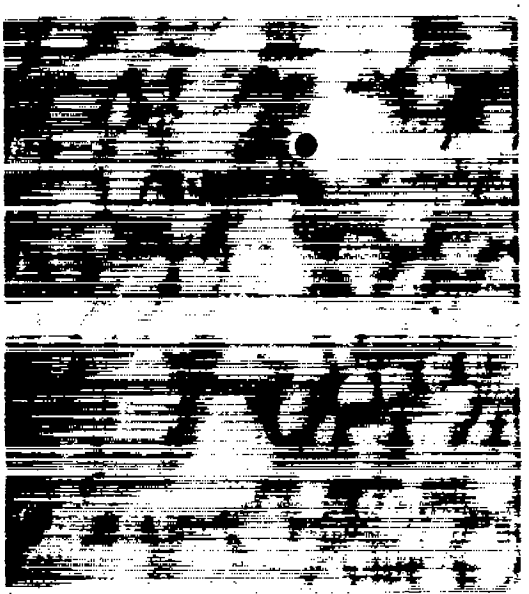

X13,000

(b) Electron micrograph.

Figure 13.- Microstructure after rupture-testing at 1,600° F and 25,000 psi when prior treatment was 2 hours at 2,150° F, furnace-cooled; hardness, 325 VPN; average rupture life, 73 hours.

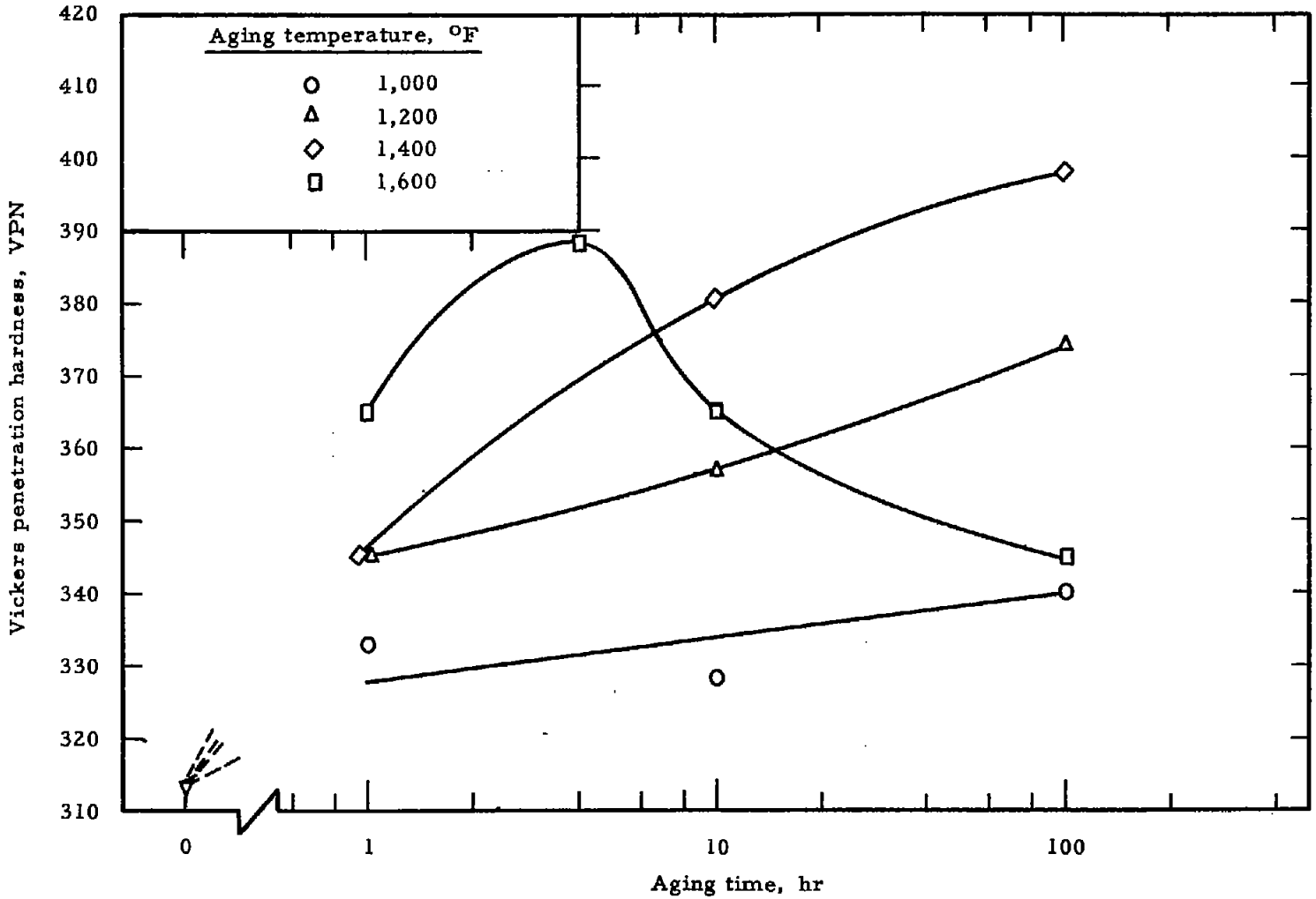

Figure 14.- Effect of aging temperature and time upon hardness. Treatment prior to aging was 2 hours at 2,150° F, then ice-brine-quenched.

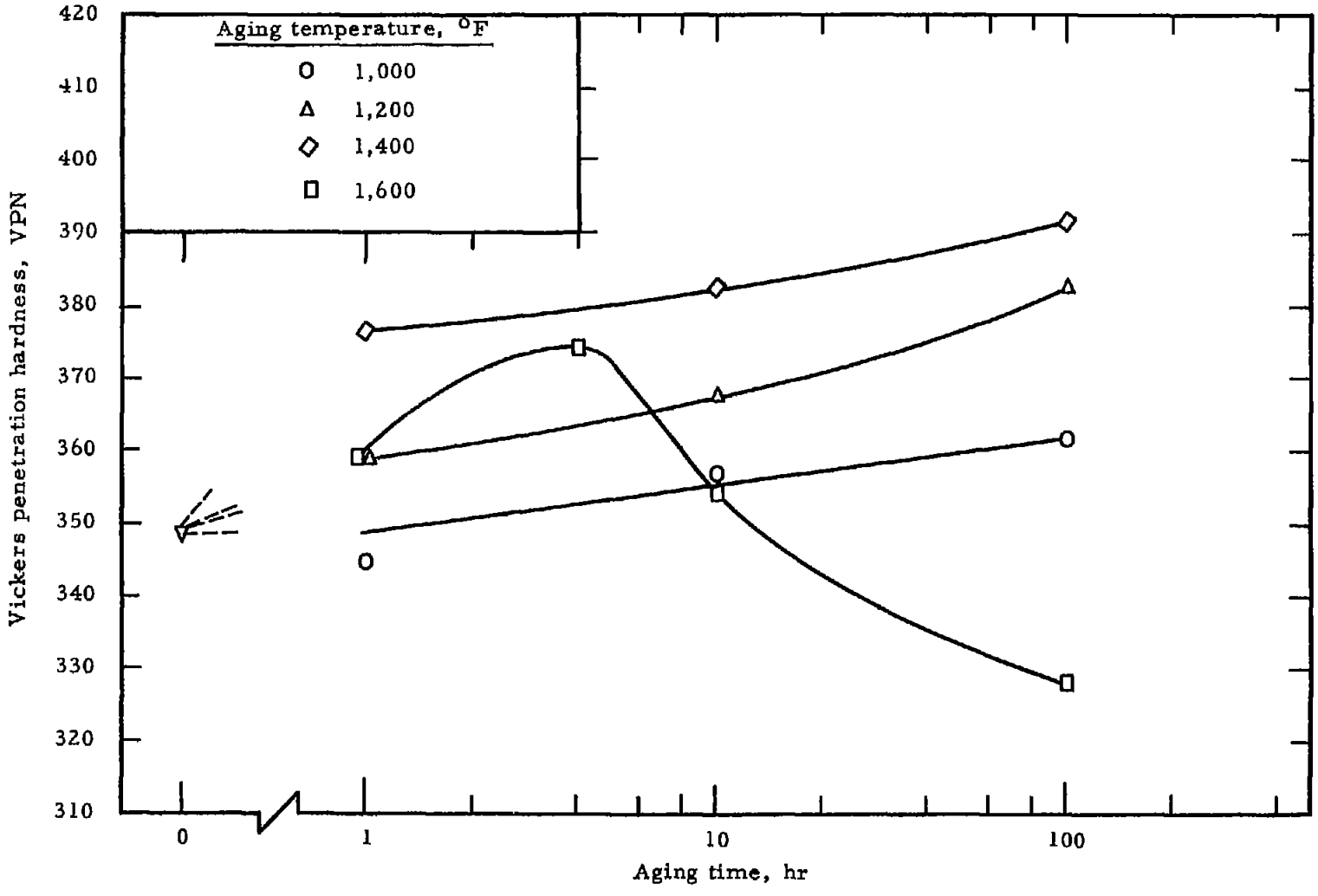

Figure 15.- Effect of aging temperature and time upon hardness. Treatment prior to aging was 2 hours at 2,150° F, then air-cooled.

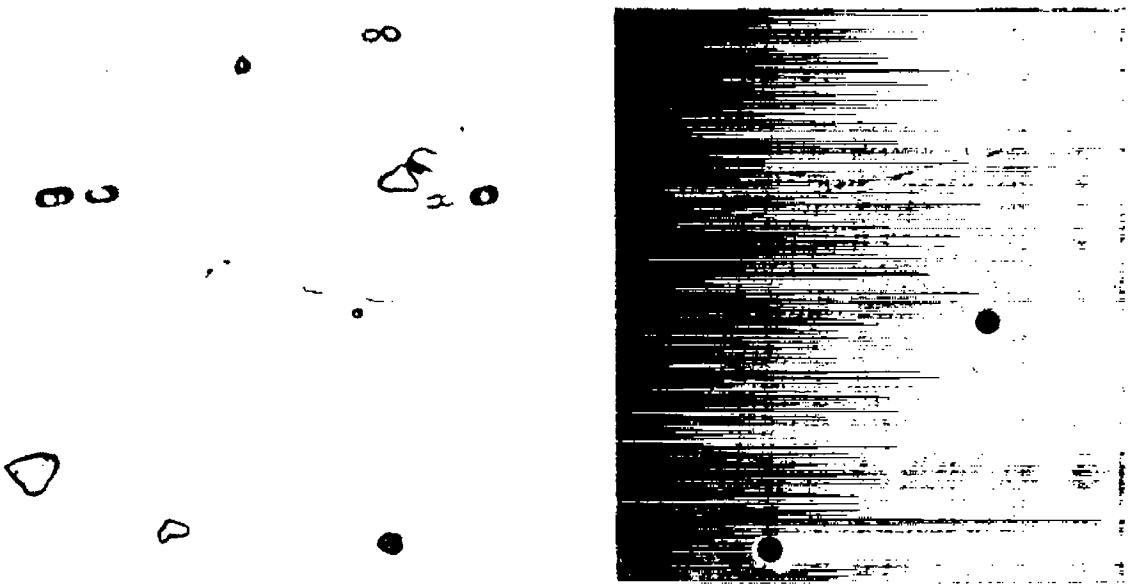

X1,000 X13,000

(a) 1,000° F; hardness, 340 VPN.

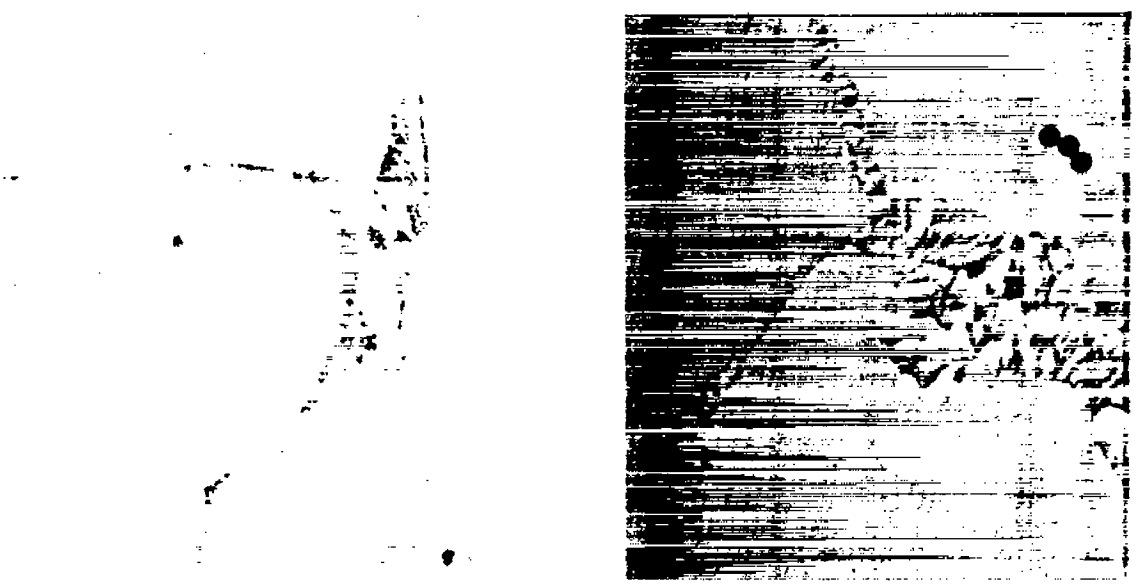

X1,000 X13,000

(b) 1,200° F; hardness, 374 VPN.

Figure 16.- Effect of aging 100 hours at designated temperatures on microstructure when initial treatment was 2 hours at 2,150° F, then ice-brine-quenched. Micrographs at X1,000 are optical micrographs; those at X13,000 are electron micrographs.

E

X1,000

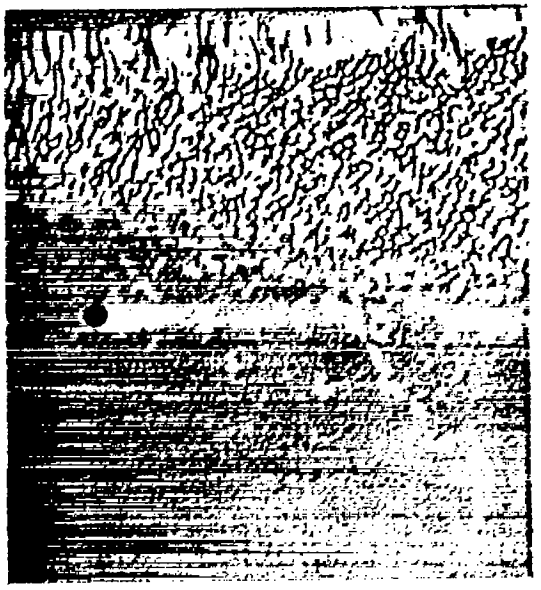

X13,000

(c) 1,400° F; hardness, 398 VPN.

X1,000

X13,000

(d) 1,600° F; hardness, 345 VPN.

Figure 16.- Concluded.

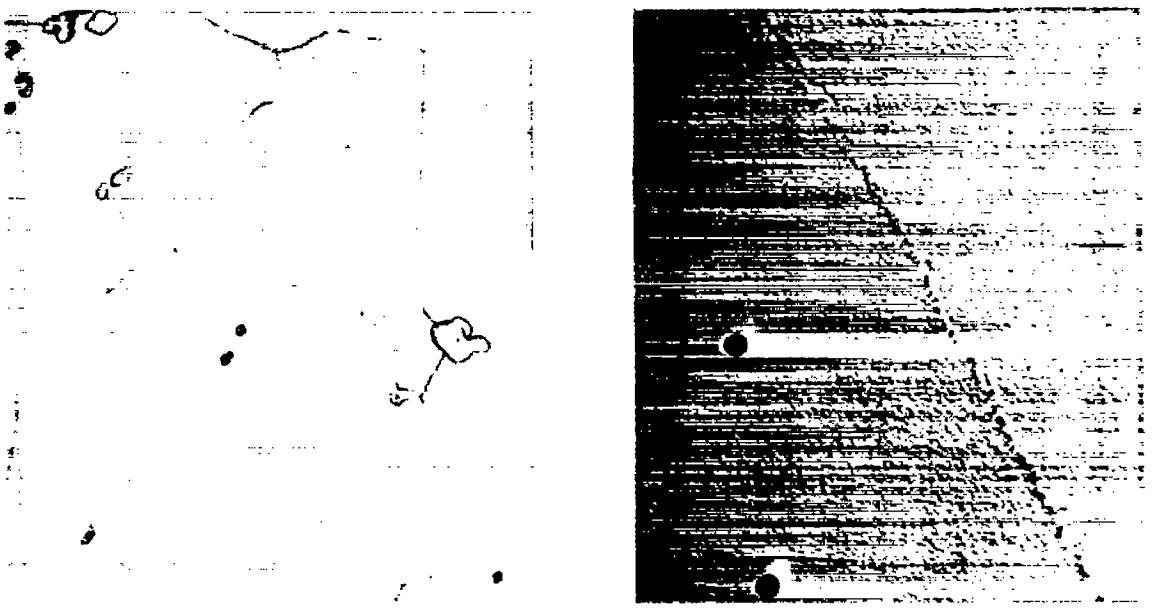

X1,000 X13,000

(a) 1,000° F; hardness, 362 VPN.

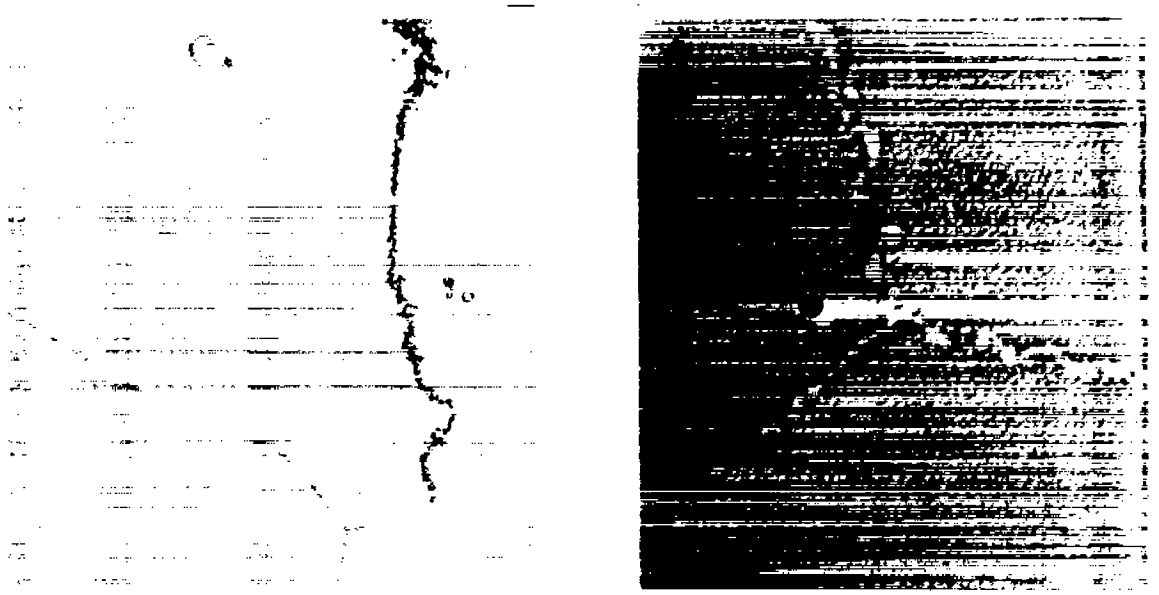

X1,000 X13,000

(b) 1,200° F; hardness, 383 VPN.

Figure 17.- Effect of aging 100 hours at designated temperatures on microstructure when initial treatment was 2 hours at 2,150° F, air-cooled. Micrographs at X1,000 are optical micrographs; those at X13,000 are electron micrographs.

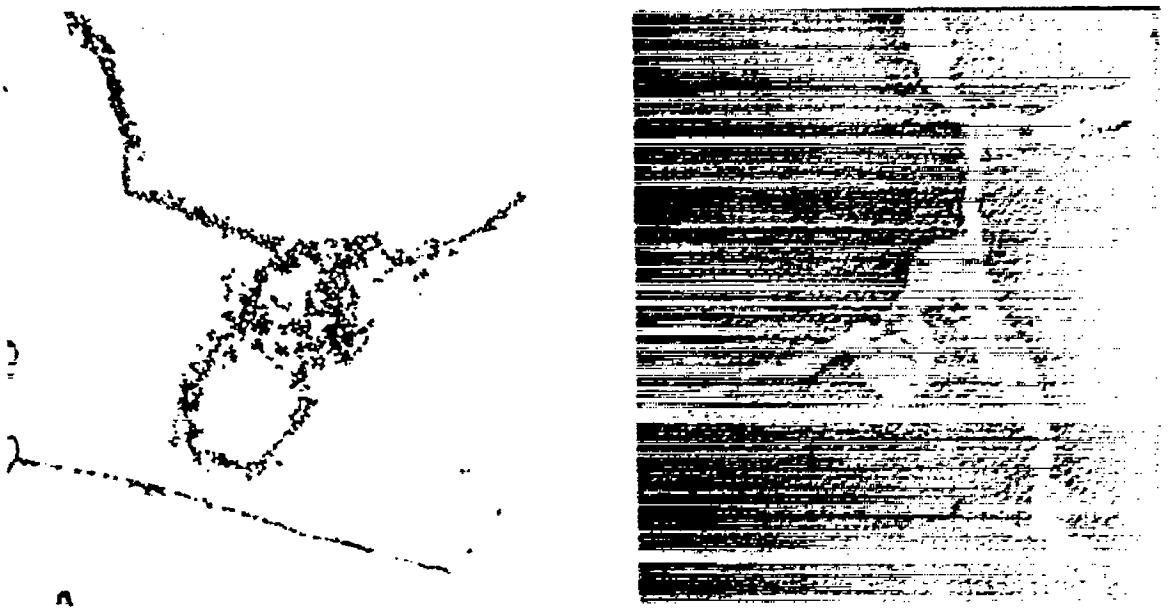

X1,000 X13,000

(c) 1,400° F; hardness, 392 VPN.

Figure 17.- Concluded.

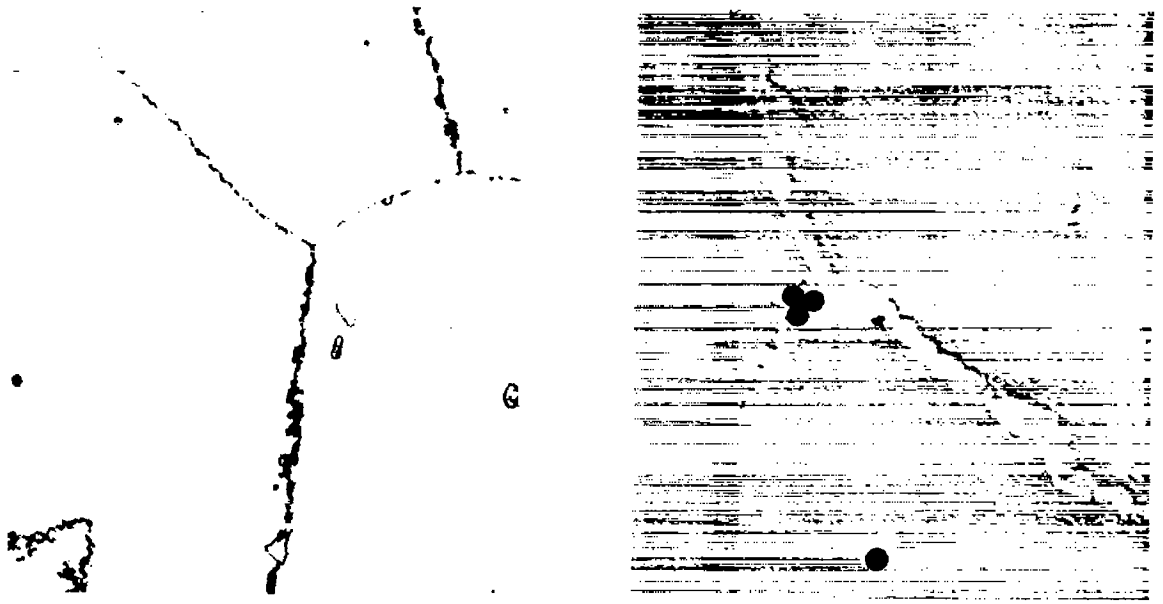

X1,000 X13,000

(a) 1 hour; hardness, 359 VPN.

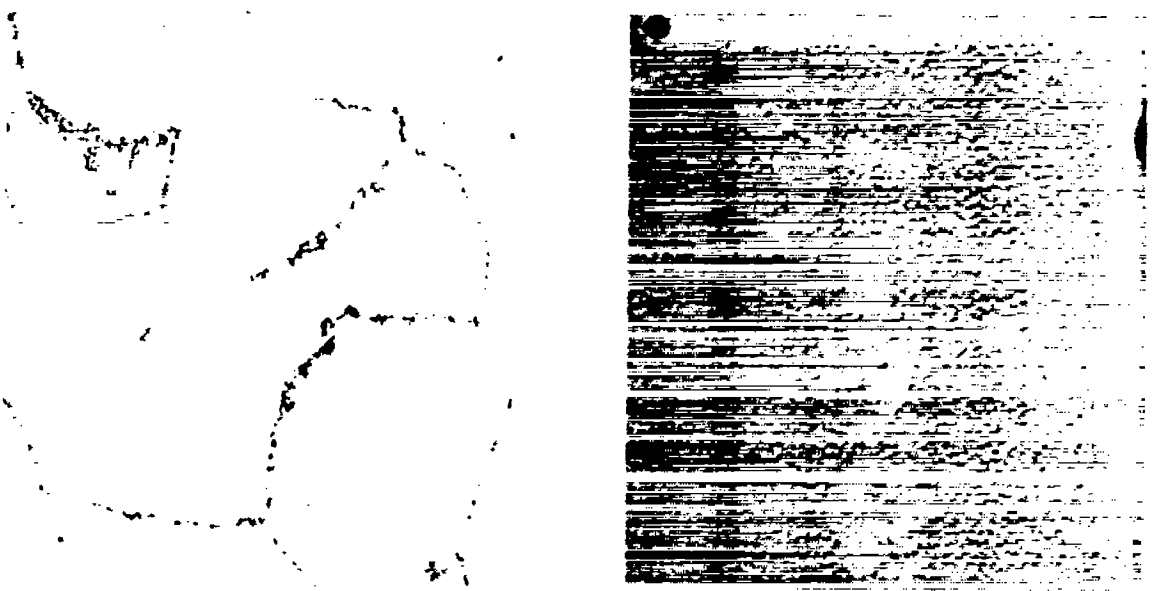

X1,000 X13,000

(b) 10 hours; hardness, 354 VPN.

Figure 18.- Effect of aging at 1,600° F for designated times on microstructure when initial treatment was 2 hours at 2,150° F, then air-cooled. Micrographs at X1,000 are optical micrographs; those at X13,000 are electron micrographs.

X1,000

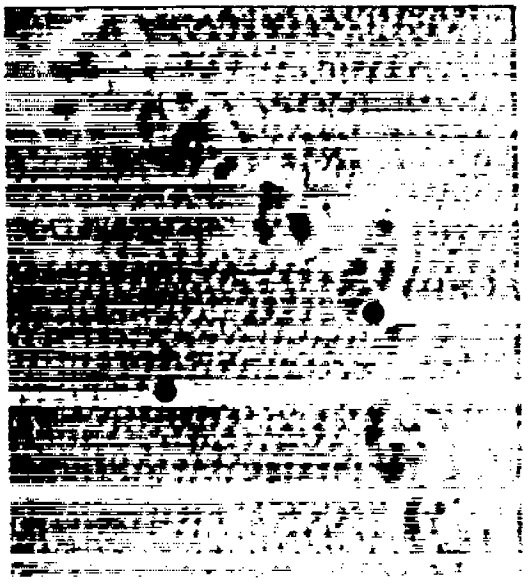

X13,000

(c) 100 hours; hardness, 328 VPN. Electron micrograph is with etchant B as were all others in report except figure 18(d).

X13,000

(d) Same time and hardness as figure 18(c) using etchant C to reveal two-phase nature of grain boundary.

Figure 18.- Concluded.

NACA - Langley Field, Va.